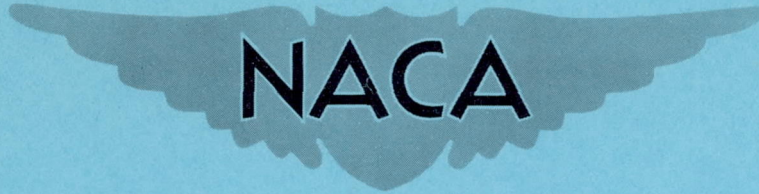


CASE FILE
COPY

RM E52G18

NACA RM E52G18



RESEARCH MEMORANDUM

ANALYTICAL PROCEDURES FOR RAPID SELECTION OF COOLANT
PASSAGE CONFIGURATIONS FOR AIR-COOLED TURBINE ROTOR
BLADES AND FOR EVALUATION OF HEAT-TRANSFER,
STRENGTH, AND PRESSURE-LOSS CHARACTERISTICS

By Robert R. Ziemer and Henry O. Slone

Lewis Flight Propulsion Laboratory
Cleveland, Ohio

NATIONAL ADVISORY COMMITTEE
FOR AERONAUTICS

WASHINGTON
September 18, 1952

NATIONAL ADVISORY COMMITTEE FOR AERONAUTICS

RESEARCH MEMORANDUMANALYTICAL PROCEDURES FOR RAPID SELECTION OF COOLANT PASSAGE
CONFIGURATIONS FOR AIR-COOLED TURBINE ROTOR BLADES AND FOR
EVALUATION OF HEAT-TRANSFER, STRENGTH, AND PRESSURE-LOSS
CHARACTERISTICS

By Robert R. Ziemer and Henry O. Slone

SUMMARY

A method based on geometric factors of the coolant passage was evolved for the rapid selection and evaluation of coolant passage configurations for air-cooled turbine rotor blades. The more promising coolant passage configurations, as selected by the simple blade evaluation criteria, are then analyzed by detailed methods to obtain absolute values of the required cooling-air weight flow, the pressure loss, and the strength characteristics.

As a verification of the simple criteria proposed for the rapid selection and evaluation of a coolant passage configuration, a comparison was made of three configurations for an air-cooled nontwisted blade designed for use on a turbojet engine with a centrifugal compressor using both the simple criteria and detailed analytical methods. The analytical and experimental blade temperatures for two different coolant passage configurations of a blade used in a turbojet engine with a centrifugal compressor were compared to determine to some degree the validity of using the one-dimensional radial-blade-temperature equation for predicting blade temperatures in the detailed analysis. As a further example of the procedure used for the selection of a suitable coolant passage configuration, the simple criteria and the detailed analytical methods were used to select a coolant passage configuration for a turbine blade to be used in a turbojet engine having an axial-flow compressor.

INTRODUCTION

In general, the requirements of a good air-cooled turbine rotor blade are high cooling effectiveness, low pressure drop, acceptable stress levels, light weight, and ease of manufacture. Methods of controlling these qualities in design are being investigated at the NACA

Lewis laboratory. The requirements for maximum cooling effectiveness have been studied through experimental investigations on a variety of coolant passage configurations for air-cooled blades. References 1 to 5 report the results of heat-transfer and endurance investigations on the more promising air-cooled shell-supported blade configurations which were tested in a production turbojet engine modified to accommodate air cooling.

At the same time, considerable effort has been expended on the development of air-cooled turbine blade fabrication techniques which would lend themselves to mass production procedures. Forming the blade shell from tubing by brazing the extended heat-transfer surfaces to the inside of the blade shell and then brazing the shell to the base appears desirable from a production standpoint (reference 6). Moreover, a blade fabricated in this manner permits extension of the cooling-air passage closer to the leading and trailing edges than was possible in cast blades such as those used in reference 4. The extension of the coolant passages aids in the reduction of the large chordwise temperature gradients formerly encountered.

As a result of the investigations of cooling effectiveness and fabrication techniques conducted on air-cooled turbine blades, satisfactory blades have been developed for use in a turbojet engine having a centrifugal compressor. For example, the tube-filled blade configuration of reference 4 was proven successful for a given blade profile in the centrifugal-flow-compressor engine. In order to reduce the experimentation and lengthy analytical computations required for the development of blades for other installations, it is desirable that a reliable method for rapid selection and evaluation of an internal coolant passage configuration for any air-cooled rotor blade be available. That is, if a number of different possible air-cooled blade configurations are to be considered for a given turbine, the more promising configurations could be rapidly selected and then be further analyzed by detailed analytical methods.

Evaluating the cooling effectiveness of cooled blades necessitates that the blade temperatures be known. Analytical equations for predicting blade temperatures for air-cooled and liquid-cooled turbine rotor blades are presented in references 7 and 8, respectively. Good agreement between analytical blade temperatures calculated by the methods presented in reference 8 is shown in references 9 and 10 for the experimental blade temperatures of a water-cooled turbine. So far as is known, however, no experimental verification of the one-dimensional blade radial temperature-distribution equation for rotating air-cooled blades as presented in reference 7 has been made, and one of the objectives of this report is concerned with this problem.

In addition to an evaluation of the cooling effectiveness of a blade, some estimate of the pressure losses is required in the analysis of cooled blades. The methods for obtaining the pressure-loss characteristics of air-cooled blades are presented in reference 11 and verified in reference 12 for two air-cooled blades tested under static conditions. Reference 12 also presents an integrated form of the differential equation of momentum presented in reference 11 that greatly reduces the labor required to evaluate the pressure changes through the blade coolant passage.

If the analysis of reference 7 is assumed applicable to air-cooled blades, the coolant passage of an air-cooled turbine rotor blade may be designed for a specific application. The procedure required to evaluate the cooling effectiveness and pressure-loss characteristics using the methods given in references 7 and 12 is time consuming, however, especially if a large number of configurations are to be considered. The stress, weight, and fabrication characteristics, which are also important factors, may be evaluated more readily. It is therefore important that a method be evolved that will give, for a specific blade profile and application, a relative evaluation of the cooling effectiveness, pressure loss, and strength characteristics of a number of coolant passage configurations in a reasonable length of time. Obtaining such a method is another objective of this report.

Since the more promising of the configurations selected by this relative evaluation will be analyzed in detail by the methods of references 7 and 12, it is necessary, as previously mentioned, to verify the reliability of the analytical temperature-distribution equation of reference 7. Consequently, a comparison has been made between the experimental and analytical blade temperatures obtained for two rotating air-cooled blade configurations which were investigated in a turbojet engine with a centrifugal compressor (references 4 and 5). This comparison utilized the experimental values of blade temperature obtained at a span position one-third from the blade base for a tube-filled blade and a finned blade with an insert. These two blades have essentially the same external profile at the one-third span position.

An analysis for the relative evaluation of the heat-transfer, strength, and pressure-loss characteristics based on certain geometric factors of the coolant passage was then made. This analysis was applied to the two coolant configurations of references 4 and 5 and to a third blade configuration having 35 fins, made of corrugated sheet metal, in the coolant passage. The relative magnitudes of these geometric factors were compared with the values obtained by the detailed analytical methods to gain an indication of the reliability of the evaluation based on the geometric factors.

As an illustration of the procedure involved in the rapid selection of a coolant passage configuration, an analysis was made to select a coolant passage configuration for an air-cooled rotor blade for the turbine of a turbojet engine with an axial-flow compressor. This blade profile was quite different from that for the engine having a centrifugal-flow compressor. An analytical comparison was first made of nine proposed coolant passage configurations for this blade shape on the basis of the geometric factors previously mentioned, and the two most promising blades were then further analyzed utilizing the detailed analytical methods in order to obtain absolute values.

Thus, the complete purpose of this report is to present (1) a comparison of experimentally measured and analytically predicted average blade temperatures for two coolant passage configurations; (2) an analytical method for the rapid selection and the evaluation of a coolant passage configuration for any air-cooled turbine rotor blade; (3) a verification of the proposed simple criteria by a comparison with the results obtained using the detailed analytical equations; and (4) an illustration of the procedure involved for the selection and evaluation of a coolant passage configuration for a particular air-cooled blade profile and application.

DETAILED ANALYTICAL METHODS FOR SELECTING AND EVALUATING

AIR-COOLED BLADES

The three principal factors that should be considered in the selection and evaluation of a coolant passage configuration for an air-cooled turbine rotor blade are (1) the heat-transfer characteristics, or the cooling effectiveness; (2) the strength characteristics, which are defined herein as a stress-ratio factor; and (3) the pressure-loss characteristics, which concern the radial static pressure variation within the coolant passage. All the procedures to be described in this section have been presented previously in NACA publications and are assembled here for convenience and to illustrate all the detailed methods used herein to evaluate coolant passage characteristics.

Critical Blade Section and Cooling-Air Flow Requirements

The heat-transfer characteristics, or cooling effectiveness, of a particular coolant passage configuration for a shell-supported blade are measured by the amount of cooling air and the cooling-air temperature required to maintain a given blade shell temperature. The determination of the required cooling-air flow necessitates the evaluation of the outside and inside heat-transfer coefficients of the blade, the

effectiveness of the internal heat-transfer surfaces, and the span position of the blade where the analytical average blade shell temperature curve is tangent to the blade shell temperature curve, which is found from a consideration of the blade centrifugal stresses and the stress-to-rupture properties of the blade material. This point of tangency will be called the critical blade section.

Analytical blade shell radial temperature distribution. - The equation which gives the one-dimensional radial temperature distribution for an air-cooled turbine blade is stated and derived in reference 7. In general, the rotational terms of the nondimensional blade temperature-distribution equation (equation (18), reference 7) are of minor importance and can be omitted. Thus, the one-dimensional equation used is

$$\frac{T_{g,e} - \bar{T}_B}{T_{g,e} - T_{a,e,h}} = \frac{1}{1 + \lambda} e^{-\left(\frac{1}{1 + \lambda} \frac{\bar{h}_o l_o x}{c_{p,a,B} w_a}\right)} \quad (1)$$

where

$$\lambda = \frac{\bar{h}_o l_o}{\bar{h}_f l_i}$$

(Definitions of symbols are given in appendix A.)

Before equation (1) can be applied to determine the blade temperatures of a given turbine, it is necessary that $T_{g,e}$, $T_{a,e,h}$, \bar{h}_o , and \bar{h}_f be known. The effective gas temperature $T_{g,e}$ can be evaluated from turbine design or operational data, equation (11) of reference 13, and the values of recovery factor presented in reference 14. The effective cooling-air inlet temperature at the blade base $T_{a,e,h}$ must be assumed on the basis of the compressor bleed temperature expected and subsequent temperature rises of the air prior to the blade base. In most cases, the total cooling-air temperature $T'_{a,h}$ can be used without introducing appreciable errors. The methods for obtaining \bar{h}_o and \bar{h}_f are now discussed.

Determination of gas-to-blade heat-transfer coefficient: In order to obtain average blade temperatures around the blade periphery for a given radial position, an average value of h_o is used in equation (1). This average outside analytical heat-transfer coefficient \bar{h}_o is given by the following correlation equation (equation (40), reference 15, in the notation used herein):

$$\frac{\overline{Nu}_{g,B}}{(\overline{Pr}_{g,B})^{\frac{1}{3}}} = \overline{F} (\overline{Re}_{g,B})^z \quad (2)$$

where \overline{F} and z are functions of ξ and Eu . For the blade under consideration, \overline{F} and z are determined from the theoretical chordwise velocity-distribution curve required to evaluate ξ and Eu , which may be obtained by applying stream filament theory derived for compressible flow around blades (reference 16) to the blade under investigation. The manner of obtaining ξ and Eu is described in appendix B of reference 15.

Determination of blade-to-coolant heat-transfer coefficient: For a blade that has internal surface in the hollow blade shell, an inside heat-transfer coefficient based on the total heat-transfer surface area and temperatures can be obtained from equation (90) of appendix F of reference 11 where in the present notation

$$\overline{h}_{a,B} = 0.019 (\overline{Re}_{a,B})^{0.8} \left(\frac{\overline{k}_{a,B}}{D_h} \right) \quad (3)$$

in which

$$\overline{Re}_{a,B} = \frac{w_a \overline{D}_h}{A_a \mu_{a,B}} \frac{\overline{T}'_a}{\overline{T}_B} \quad (4)$$

As indicated, the fluid properties in equations (4) and (5) are based on blade temperature. It can be shown (reference 17) that for air flowing in a smooth round tube, a satisfactory correlation of average inside heat-transfer coefficients was obtained for a range of wall temperatures from approximately 150° to 1600° F and an inlet-air temperature near 75° F when the fluid properties were based on wall temperatures. Therefore, for the accuracy required in this investigation, fluid properties based on blade temperature are satisfactory. The average cooling-air temperature \overline{T}'_a required in equation (4) is obtained by determining a cooling-air temperature distribution through the blade from equations reported in reference 11 with a known value of $T_{a,e,h}$. For this analysis, \overline{T}'_a is taken as the average of the cooling-air temperatures at the blade root and blade tip.

The average effective inside heat-transfer coefficient \overline{h}_f required in equation (1) is based only on wall temperature and wall surface area.

The following equation (equation (6), reference 7, in the notation of this report) gives the relation between \bar{h}_F and $h_{a,B}$ for a finned blade having fins that are nearly uniform:

$$\bar{h}_F = \frac{\bar{h}_{a,B}}{m + \tau} \left[\frac{2L \tanh(L\phi)}{L\phi} + m \right] \quad (5)$$

where

m fin spacing

τ fin thickness

L effective fin length

$$\phi = \sqrt{\frac{2 \bar{h}_{a,B}}{\tau k_B}}$$

When equation (5) is applied to blades having fins of varying lengths or internal heat-transfer surfaces of varying shapes, it is desirable that the internal surface be broken up into sections of equivalent fins rather than that an average fin length be used in equation (5). It can be shown that for "n" sections of equivalent fins, each of which contains α_ζ fins, equation (5) becomes

$$\bar{h}_F = \sum_{\zeta=1}^n \frac{\bar{h}_{a,B}}{\alpha_\zeta (m_\zeta + \tau_\zeta)} \left[\sum_{\zeta=1}^n \frac{\alpha_\zeta 2L_\zeta \tanh(L_\zeta \phi_\zeta)}{L_\zeta \phi_\zeta} + \sum_{\zeta=1}^n \alpha_\zeta m_\zeta \right] \quad (6)$$

where ζ is the index of summation.

The application of equation (6) to air-cooled turbine blades having internal surfaces other than fins, such as tubed or corrugated blades, requires that the internal surface be replaced by equivalent fins. The following method is therefore suggested for use in conjunction with equation (6):

- (1) By inspection, divide the blade into "n" sections of equivalent fins which appear to have equal fin lengths, spacings, and thicknesses, and determine the number of fins α_ζ in each section.

- (2) For each section, determine the inside blade shell perimeter $l_{i,\zeta}$ and the total wetted perimeter $l_{W,\zeta}$.
- (3) Determine the quantities required for equation (6) according to the following definitions:

The inside blade shell perimeter is

$$l_{i,\zeta} = \alpha_{\zeta} (m_{\zeta} + \tau_{\zeta}) \quad (7)$$

Now, since α_{ζ} is known and τ can be easily determined (for fins or corrugations, thickness of fins or corrugations; for tubes, wall thickness of tubes), equation (7) may be written

$$\alpha_{\zeta} m_{\zeta} = l_{i,\zeta} - \alpha_{\zeta} \tau_{\zeta} \quad (8)$$

and the fin length for a particular section is

$$L_{\zeta} = \frac{l_{W,\zeta} - \alpha_{\zeta} m_{\zeta}}{2\alpha_{\zeta}} \quad (9)$$

Therefore, for any air-cooled blade that has internal surface in the hollow blade shell, the blade thermal conductivity and equations (7) to (9) are used in conjunction with equation (6) to obtain a value of \bar{h}_f for a particular value of $\bar{h}_{a,B}$. An example of the application of equations (6) to (9) to both a corrugated and a tubed type blade is given in appendix B.

Determination of blade critical section. - As previously mentioned, the blade critical section is the span position where a blade radial temperature-distribution curve (hereinafter designated Curve 1) determined by means of equation (1) is tangent to the blade shell radial temperature-distribution curve (hereinafter designated Curve 2) determined by use of the blade centrifugal stress and the stress-to-rupture properties of the blade material. The centrifugal-stress distribution is determined by calculating the stress from the tip to the root of the blade (see fig. 1(a)). The method for determining this centrifugal stress is given in equation (2) of reference 13. When the centrifugal-stress distribution is known, the blade shell radial temperature distribution (Curve 2) for determining the blade critical section can be determined from the blade material stress-to-rupture data (see fig. 1(b)) and plotted as shown in figure 1(c). The radial blade temperature

distribution (Curve 1) is determined for a number of cooling-air weight flows and plotted on the same coordinates until a point of tangency is determined between one of these analytical curves and the blade shell temperature curve (Curve 2). This point on the blade span is called the critical section.

Stress-Ratio Factor

A method for comparing and evaluating the cooling effectiveness of air-cooled turbine rotor blades of different configurations on the basis of a stress-ratio factor is reported in reference 4. For air-cooled turbine rotor blades with chordwise temperature gradients (fig. 2(a)), plastic flow would occur and a portion of the load would be transferred to a section of the blade that is still in the elastic range even though parts of the blade are operating beyond the elastic limit of the material. The local allowable chordwise stresses are evaluated from the blade temperatures and the stress-to-rupture properties of the blade material used (fig. 2(b)). The allowable stress for the blade at the critical blade section is then assumed to be the integrated average of the local allowable stresses. On the basis that the centrifugal stress is the most significant in defining the actual operating stresses in the turbine rotor blade, the stress-ratio factor is defined as

$$\text{Stress-ratio factor} = \frac{\text{area under allowable stress curve}}{\text{area under actual centrifugal stress curve}}$$

(see fig. 2(b)). Therefore, once the critical blade section for a particular blade has been determined, the allowable stresses may be obtained for a range of cooling-air flow ratio. These allowable stresses are then used in conjunction with the centrifugal stress obtained at the critical blade section to determine stress-ratio factors for a range of cooling-air flow ratio. A stress-ratio factor is then assumed for determining a minimum value of cooling-air flow ratio.

Stress-ratio factors based on analytical blade temperatures are determined in the following manner:

- (1) Determine the blade shell radial temperature distribution (Curve 2) for the blade under consideration.
- (2) Calculate the average peripheral blade temperature from equation (1) for a range of cooling-air flow ratio for a series of radial stations (Curve 1).
- (3) Plot the blade shell temperature distribution as determined from blade material stress-to-rupture data (Curve 2) and the radial

blade temperature distributions (Curve 1) on the same coordinates and obtain a point of tangency between one of the blade temperature-distribution curves (Curve 1) and the blade shell distribution curve (Curve 2). The radial blade position at which this point of tangency occurs is assumed to be the critical blade section (see fig. 1(c)).

- (4) Use the average peripheral blade temperatures occurring at the critical blade section and the blade stress-to-rupture data to obtain an average allowable stress for each of the cooling-air flow ratios considered. (Since an average blade temperature is used, it is not possible to obtain an integrated allowable stress based on a peripheral temperature distribution.)
- (5) Calculate the average centrifugal stress at the critical blade section.
- (6) Divide the average allowable stress at a given cooling-air flow ratio by the average centrifugal stress and thus determine a stress-ratio factor for the given cooling-air flow ratio.

Pressure-Loss Characteristics

Once the required cooling-air flow ratio for a given stress-ratio factor has been determined, the required cooling-air static pressure at the blade root may be calculated from the following equations (equations (1) and (11), reference 12, in the present notation):

$$\frac{p_{a,h}}{p_{a,T}} = \frac{A_{a,T}}{A_{a,h}} \frac{M_{a,T}}{M_{a,h}} \sqrt{\frac{T'_{a,h}}{T'_{a,T}} \left(\frac{1 + \frac{\gamma_a - 1}{2} M_{a,T}^2}{1 + \frac{\gamma_a - 1}{2} M_{a,h}^2} \right)} \quad (10)$$

and

$$\frac{1}{M_{a,h}^2} = \frac{1}{M_{a,T}^2} + 1.2 \ln \frac{M_{a,T}^2}{M_{a,h}^2} \left(\frac{1 + 0.2 M_{a,h}^2}{1 + 0.2 M_{a,T}^2} \right) + \frac{4f_b \gamma_a}{D_h} + \gamma_a \ln \frac{T'_{a,T}}{T'_{a,h}} +$$

$$\frac{T'_{a,T} - T'_{a,h}}{\Phi \omega} \left(\frac{1}{M_{a,T}^2} \right)_m - \frac{2\omega^2 r_h b}{gR} \left(1 + \frac{\gamma_a - 1}{2} M_a^2 \right)_m \frac{1}{\Phi \omega} \left(\frac{1}{M_{a,T}^2} \right)_m \left(1 + \frac{b}{r_h} \psi \right) \quad (11)$$

where

$$\left(\frac{1}{M_a^2 T_a'}\right)_m = \frac{1}{2} \left[\left(\frac{1}{M_a^2 T_a'}\right)_h + \left(\frac{1}{M_a^2 T_a'}\right)_T \right]$$

and

$$\left(1 + \frac{\gamma_a - 1}{2} M_a^2\right)_m = \frac{1}{2} \left[\left(1 + \frac{\gamma_a - 1}{2} M_{a,h}^2\right) + \left(1 + \frac{\gamma_a - 1}{2} M_{a,T}^2\right) \right]$$

The cooling-air total temperature at the blade tip required in equations (10) and (11) may be calculated from equations presented in reference 11 with a known value of $T_{a,h}'$. The equation parameters φ_ω and ψ as well as methods for determining $P_{a,T}$, $M_{a,T}$, and f are presented in reference 12.

SIMPLE ANALYTICAL CRITERIA FOR SELECTING AND EVALUATING

AIR-COOLED BLADES

The selection and evaluation of several coolant passage configurations for a blade with a specific application by the detailed analytical methods just described is a rather long and involved process. It is desirable that a more rapid method for the relative evaluation of a number of coolant passage configurations for a given blade be available. Such a method, based on certain geometric factors of the coolant passage configurations, has been evolved. The coolant flow area and the internal cooled surface area are the criteria used to evaluate the cooling effectiveness of the coolant configurations; the volume of the airfoil and the cross-sectional metal area are used for the blade weight and stress criteria; and the hydraulic diameter of the coolant passage gives an indication of the cooling-air pressure losses. A number of coolant passages for a specific blade can be investigated quite rapidly by the use of these geometric factors, and then the absolute evaluation of the more promising configurations can be made by the detailed methods just described.

Blade Cooling Effectiveness Criterion

Since for a specific blade shape and application the outside heat-transfer coefficient remains constant, the factors influencing the cooling effectiveness of a blade are the inside heat-transfer coefficient and the effectiveness of the internal heat-transfer surface area. Combining equations (3) and (4) shows that

$$\bar{h}_{a,B} = 0.019 \left(\frac{w_a \bar{D}_h}{\bar{A}_a \bar{\mu}_{a,B}} \right)^{0.8} \left(\frac{\bar{T}'_a}{\bar{T}_B} \right)^{0.8} \left(\frac{\bar{k}_{a,B}}{\bar{D}_h} \right) \quad (12)$$

With $\bar{\mu}_{a,B}$ and $\bar{k}_{a,B}$ assumed constant, equation (12) can be written

$$\bar{h}_{a,B} = K \left(\frac{w_a \bar{D}_h}{\bar{A}_a} \right)^{0.8} \left(\frac{\bar{T}'_a}{\bar{T}_B} \right)^{0.8} \left(\frac{1}{\bar{D}_h} \right) \quad (13)$$

The total amount of heat transferred to the cooling air passing through the blade is given by

$$Q = \bar{h}_{a,B} S_{i,t} (\bar{T}_{B,t} - \bar{T}'_a) = \bar{h}_o S_o (T_{g,e} - \bar{T}_B) \quad (14)$$

where $\bar{T}_{B,t}$ is the average temperature of the inside wetted surface and \bar{T}_B is the average temperature of the blade shell. Substituting equation (13) into the first part of equation (14) gives

$$Q = K \left(\frac{w_a \bar{D}_h}{\bar{A}_a} \right)^{0.8} \left(\frac{\bar{T}'_a}{\bar{T}_B} \right)^{0.8} \left(\frac{1}{\bar{D}_h} \right) S_{i,t} (\bar{T}_{B,t} - \bar{T}'_a) \quad (15)$$

With the hydraulic diameter defined as $4\bar{A}_a b / S_{i,t}$, equation (15) can be written

$$Q = K' (w_a)^{0.8} \left(\frac{S_{i,t}^{1.2}}{\bar{A}_a} \right) \left(\frac{\bar{T}'_a}{\bar{T}_B} \right)^{0.8} (\bar{T}_{B,t} - \bar{T}'_a) \quad (16)$$

It can also be shown that $(\bar{T}_a / \bar{T}_B)^{0.8} (\bar{T}_{B,t} - \bar{T}'_a)$ is a function of $(w_a)^\theta$, where the exponent θ is negative but less than 0.8. Thus, equation (16) can be written

$$Q = K'' (w_a)^{0.8} (w_a)^\theta \left(\frac{S_{i,t}^{1.2}}{\bar{A}_a} \right) \quad \left. \vphantom{Q = K'' (w_a)^{0.8} (w_a)^\theta \left(\frac{S_{i,t}^{1.2}}{\bar{A}_a} \right)} \right\} \quad (17)$$

or

$$Q = K''' (w_a)^\beta \left(\frac{S_{i,t}^{1.2}}{\bar{A}_a} \right)$$

where the exponent β is positive.

The higher the ratio $(S_{i,t})^{1.2}/\bar{A}_a$ to dissipate a given amount of heat Q , which is essentially constant except for small changes in the average blade temperature, the smaller is the required cooling-air flow. The cooling effectiveness of a configuration is increased as the required cooling-air flow is decreased. The ratio $(S_{i,t})^{1.2}/\bar{A}_a$ therefore is the criterion to be considered for the cooling effectiveness of an air-cooled blade.

Blade Stress and Weight Criteria

For a specific application of a blade shell having a given spanwise variation in the blade wall thickness, wherein it is assumed that the blade shell and internal heat-transfer surfaces support themselves separately, it can be shown that the centrifugal stress at any blade span position is a function of the ratio of the cross-sectional metal area of the blade at the blade tip to the cross-sectional metal area of the blade at the specified span position. Therefore, in order to obtain a relative indication of the centrifugal stresses of a particular blade shell having various coolant passage configurations, it is necessary only to compare the ratios of the cross-sectional metal areas at the blade tip with the cross-sectional metal areas of the blades at the desired span position. Essentially, this comparison is simply a comparison of the taper ratios of the blades. For simplicity, however, especially when the relative merits of a particular tapered blade shell having a number of different constant-area coolant passage configurations are desired, a relative comparison of the centrifugal stresses may be obtained by considering the ratio of the cross-sectional metal area of the tapered member (blade shell) to the cross-sectional metal area of the untapered members (coolant passage configurations) at a particular span position. This comparison is usually made at the blade root where the stress is the greatest and drawings of the blade under consideration are usually available. The larger this ratio A_{tap}/A_{untap} is, the smaller is the centrifugal stress. For example, a tapered blade shell having no internal heat-transfer surface (hollow air-cooled blade) would have a ratio of infinity at the blade root, whereas the same blade shell having fins in the coolant passage might have a ratio equal to five. Therefore, the hollow blade would have the smaller centrifugal stress of the two blades. If the blade shell has no taper (A_{tap}/A_{untap} is zero), the untapered blade shell will have the same stress at a particular span position regardless of the coolant passage configuration. It is to be pointed out, however, that this simple criterion for a relative indication of the blade stress is dependent on only the blade centrifugal force and does not necessarily indicate the stress-ratio factor since the stress-ratio factor combines the effect of both stress level and cooling effectiveness. As a consequence, this criterion can be considered only as a preliminary indication of blade strength, and an evaluation of the stress-ratio factor to obtain the effects of cooling is necessary in the final analysis.

The volume of metal in the airfoil section gives a direct measurement of the relative weight of the various configurations. Lightweight blades are important in that less metal is required in the blades themselves and because the rim loading on the disk is reduced, the disk structure can usually be lightened considerably.

Blade Pressure-Loss Criterion

The determination of the static pressure at the blade base by use of equations (10) and (11), although they are considerably shorter than the original equations reported in reference 11, is rather lengthy if a large number of coolant passage configurations are to be investigated. An examination of equations (10) and (11) and the equation in reference 11 for the temperature rise of the cooling air indicates that for a given blade profile and application the primary variables affecting the cooling-air pressure variation are the coolant flow area, the cooled surface area, the friction factor, and the hydraulic diameter. With the friction factor assumed a function of Reynolds number and the Reynolds number for a constant weight flow assumed expressible as a function of the coolant flow area and the hydraulic diameter, it appears that the hydraulic diameter (which can be expressed in terms of the coolant flow area and the cooled surface area) can be used as a criterion for the relative evaluation of the cooling-air pressure losses as long as the coolant flow areas are of approximately the same magnitude. As the hydraulic diameter becomes larger, the pressure losses would tend to decrease. For configurations which tend to have a pressure rise through the blades, as \bar{D}_h becomes larger the amount of pressure rise increases, which is a decreased pressure loss.

PROPOSED GENERAL COOLANT PASSAGE DESIGN METHOD

A proposed design method for the selection of a coolant passage configuration for any air-cooled turbine rotor blade utilizes both the detailed analytical methods and the simple analytical criteria just described. With a given blade profile and turbine operating conditions, a relative evaluation of a number of coolant passage configurations can be made utilizing the criteria described in the simplified analysis. From large cross-sectional layouts of the various coolant passage configurations to be considered, the geometric factors involved in the simple analytical criteria are evaluated. These factors are: (1) coolant flow area \bar{A}_a , (2) total cooled surface area $S_{i,t}$ (which is the wetted inside perimeter l_w multiplied by the blade span b), (3) volume of metal in the airfoil section, (4) cross-sectional metal area of the tapered member of the blade A_{tap} , (5) cross-sectional metal area of the untapered members of the blade A_{untap} , and (6) hydraulic diameter of the coolant passage \bar{D}_h .

The configuration with the highest cooling effectiveness, that is, the blade which will require the least amount of cooling air to maintain a given blade temperature, will be the blade which has the highest value of the criterion $(\dot{S}_{i,t})^{1.2}/\bar{A}_a$. The blade lightest in weight will be that with the smallest metal volume. The configuration with the highest value of $A_{\text{tap}}/A_{\text{untap}}$ will have the lowest centrifugal stress at the blade root. The largest hydraulic diameter \bar{D}_h will indicate the coolant passage configuration with the smallest pressure losses. It is quite probable that one blade coolant passage configuration will not have the best values for all the criteria considered and some compromises will be necessary.

The most promising of the coolant passage configurations as determined by the simple analytical criteria then must be further analyzed by the detailed analytical methods to obtain absolute values of the required cooling-air weight flow, the pressure loss, and the strength characteristics.

PROCEDURE USED TO VERIFY SIMPLE BLADE EVALUATION CRITERIA

Experimental Verification of Detailed Analytical Procedure

The basic equations for the evaluation of the pressure-loss characteristics of air-cooled turbine blades have been verified for two air-cooled blade configurations investigated in a static cascade (reference 12). Although the equations as presented herein are for a rotating blade and experimental verification for the rotating case has not as yet been obtained, the equations are believed applicable.

The use of the stress-ratio factor as a criterion for the strength characteristics of air-cooled blades is reported in reference 4 in which it is shown to be an improved method of comparing and evaluating air-cooled turbine blades having different temperature gradients (chordwise) and different coolant passage configurations and fabricated from different materials.

In order to determine to some degree the validity of using the one-dimensional radial-blade-temperature equation for predicting blade temperatures, a comparison was made of the analytical blade temperatures and the experimental rotor blade temperatures obtained in a turbojet engine reported in references 4 and 5. The experimental blade temperatures were obtained on blades of profile 1 (fig. 3(a)) of configurations A and B (see table I). The blade temperatures compared are the average blade temperatures at approximately the 1/3-span position, which is the region where air-cooled blades generally fail. To obtain

this average temperature from the experimental results, the measured blade temperatures at a number of chordwise positions at the 1/3-span position were plotted in the form of a temperature-difference ratio $(T_{g,e} - T_B) / (T_{g,e} - T_{a,e,h})$ (reference 1) against the blade periphery for several cooling-air flow ratios, and integrated average temperature-difference ratios were obtained. The effective gas temperature and the effective cooling-air inlet temperatures assumed for the analysis were used to evaluate the average blade temperatures for the cooling-air flow ratios considered. Then the allowable stress used in both the stress-ratio factors based on analytical temperatures and the stress-ratio factors based on experimental blade temperatures were evaluated on the basis of an average blade temperature, whereas in references 4 and 5 the stress-ratio factors are based on an integrated allowable stress determined from a chordwise temperature-distribution curve. The difference between these two methods of determining stress-ratio factors is dependent on the nonlinearity of the stress-to-rupture curve for the blade material under consideration. In most cases this difference is small. For example, at a cooling-air flow ratio of 0.02 the stress-ratio factor based on an integrated allowable stress determined from experimental chordwise blade temperatures and a stress-ratio factor based on an experimental average blade temperature are 3.0 and 3.1, respectively, for configuration A of this report.

The insert blade with fins of reference 5 was a twisted blade, whereas configuration B, profile 1, of this report is considered to be nontwisted. The profiles of the blades, however, are practically identical. It was assumed, for the purpose of this analysis, that the effect of this twist would be negligible in the evaluation of the outside heat-transfer coefficient at the blade span position considered.

Verification of Simple Criteria for Three Coolant

Passage Configurations of Profile 1

Although the development of the criteria for the rapid selection of a coolant passage configuration is evident from the equations involved for the cooling effectiveness and the centrifugal stress, the case of the hydraulic diameter for describing the pressure-loss characteristics is not so well defined. As a verification of the criteria proposed, a comparison was made of three coolant passage configurations for an air-cooled nontwisted blade designed for use in a turbojet engine with a centrifugal compressor (see fig. 3(a) for blade profile) using both the simple criteria and the detailed analytical methods.

Blade aerodynamic design. - In the design of the aerodynamic profile for turbine rotor blades suitable for air cooling, several problems not considered in most turbine rotor blade designs were introduced. To provide adequate cooling of the blades with the type of internal heat-transfer surfaces used, it was necessary that the blade leading and trailing edges be sufficiently large. For fabrication simplicity, it was advantageous for the rotor blade to have no aerodynamic twist along the radius and for the coolant passage to be of constant cross section from root to tip. To aid in investigating these problems, a nontwisted rotor blade of uniform camber was designed for the turbojet engine with the centrifugal compressor on the basis of the analysis of reference 18. The solidity, aspect ratio, and axial chord were maintained the same as for the original uncooled turbine, but the blade profile was altered to provide a straight, constant-area cooling-air passage within the blade. In the design of the twisted turbine stator blades for the centrifugal engine, the solidity, aspect ratio, axial chord (at the mean section), blade height, and leading- and trailing-edge radii of the original turbine were maintained. The profile derived is shown in figure 3(a).

Coolant passage configurations. - A total of three coolant passage configurations was considered for the turbine blade for the turbojet engine with the centrifugal compressor (see table I). A 10-tube blade, configuration A, an insert blade with fins, configuration B, and a finned blade, configuration C, were first analyzed by the simple criteria and then checked by the detailed analytical methods. Comparisons were made of the three coolant passage configurations on the basis of analytical blade temperatures, stress-ratio factors, cooling-air static pressure variations, and blade weight.

Illustration of Selection of Coolant Passage Configuration for Profile 2 Using Simple Criteria

As an example of the method described in a preceding section, the selection of a coolant passage configuration for a turbine blade for application in a turbojet engine having an axial-flow compressor (see fig. 3(b), profile 2), which is quite different in aerodynamic profile from that for the engine with the centrifugal compressor, is presented.

Blade aerodynamic design. - The conservative aerodynamic loading and centrifugal stresses of the turbine of the axial-flow-compressor engine offered opportunities for a drastic revision of the entire turbine design to reduce the number of blades to be cooled, decrease the rim loading on the disks, and increase the scale of the blade coolant passage so that more uniform cooling and increased producibility could be achieved. To accomplish this, the number of blades was reduced from 96 to 72, but the solidity was maintained constant by increasing the

axial chord of the blade from 1.68 inches to 2.27 inches. The rotor blade height was maintained constant. Because of the low tip speed and large diameter of this particular turbine, it seemed that, in addition to the constant-area coolant passage, the outside aerodynamic profile could also be maintained constant from root to tip. This resulted in a blade with no taper, which should facilitate the fabrication procedures. The centrifugal stresses at the blade root of this constant cross-section shell were not prohibitive. The twisted stator blades were designed on the same basis as those for the centrifugal-flow-compressor engine. The design procedures and the results of a performance investigation of a scale model of the axial-flow-compressor engine turbine stator and rotor blades (profile 2) in cold air are presented in reference 19.

Coolant passage configurations. - Nine coolant passage configurations were considered for the turbine rotor blade of the axial-flow-compressor engine (fig. 3(b)). These configurations (see table II) were first analyzed utilizing the criteria based on the geometric factors, and the two most promising configurations were then analyzed by the detailed methods to determine the average effective inside heat-transfer coefficients. The minimum cooling-air flow requirements were then evaluated for the insert blade with fins (fig. 4) for a cooling-air inlet temperature of 180° F using the one-dimensional radial blade temperature-distribution equation, and the required cooling-air pressure at the blade root for this condition as well as the variation of stress-ratio factor with cooling-air flow ratio was determined.

Engine Conditions Affecting Cooling Requirements

The analyses reported herein were made at sea-level static engine conditions for both the centrifugal-flow-compressor engine (profile 1) and the axial-flow-compressor engine (profile 2). The values used in the analyses for determining the cooling requirements are given in table III.

RESULTS AND DISCUSSION

Experimental Verification of Detailed Analytical Procedure

Since experimental blade temperatures were available for configurations A and B of profile 1 (references 4 and 5) at a position of $1\frac{7}{16}$ inches from the blade root, a comparison was made between theory and experiment on the basis of average blade temperatures over a range of cooling-air flow ratio to verify the use of the one-dimensional radial blade-temperature equation. A comparison was also made between

the stress-ratio factors based on average analytical blade temperatures and integrated experimental blade temperatures to determine the significance of differences between these two temperatures on the stress-ratio factor. Figure 5 presents the comparison between analytical and experimental average blade temperatures for cooling-air flow ratios up to 0.04. A cooling-air inlet temperature of 180° F was used for all cases.

For configuration A (fig. 5(a)) and configuration B (fig. 5(b)), the experimental blade temperatures at the span position investigated compared quite favorably with the analytical results over the cooling-air flow ratio range investigated. In both cases, the experimental blade temperatures averaged approximately 40° to 60° F above the analytical blade temperatures. The analytical results will usually indicate lower blade temperatures than the experimental results, for in the theory the contact between the internal heat-transfer surfaces and the blade shell was assumed perfect. This is not the case for the blades used in the experimental investigations. Figure 3 of reference 4 shows that the thermal bond between the tubes in the coolant passage and the blade shell was approximately 50 percent of that desired. If the contact had been perfect, as was assumed in the analytical analysis, the experimental blade temperatures would have been lower. No attempt has been made in the analytical analysis to account for poor thermal bond between a portion of the internal heat-transfer surface and the blade shell.

Figures 6(a) and 6(b) present a comparison between analytical and experimental average blade temperatures for configurations A and B of profile 1 on the basis of stress-ratio factor as a function of cooling-air flow ratio. The stress-ratio factor was determined from the blade temperatures at a span position $1\frac{7}{16}$ inches from the blade root and the cooling-air inlet temperature was assumed to be 180° F. The results based on experimental temperatures showed good agreement with those based on analytical calculations, but the significance of the 40° to 60° F difference between the analytical and experimental results should be noted. In figure 6(a), configuration A, for a stress-ratio factor of 2.0, the analytical results indicated that a cooling-air flow ratio of 0.012 was required, but experiment showed that a cooling-air flow ratio of 0.015 was necessary to obtain the same stress-ratio factor. Thus, the actual cooling-air flow ratio was approximately 25 percent greater than the theory indicated. This again was due to the fact that in the blade temperature range considered, the stress-to-rupture data of the material used (Timken alloy 17-22A(S)) decreased rapidly with rupture temperature. A slight increase in blade temperature (40° to 60° F) represented a large decrease in allowable blade stress, which is

used in the determination of the stress-ratio factor, and thus for a given cooling-air flow ratio a lower stress-ratio factor was obtained. Conversely, to maintain a given stress-ratio factor, the actual cooling air required was greater than that indicated by theory.

As mentioned previously, the pressure-loss equations (11) and (12) were verified in a static cascade and the results reported in reference 12. The use of the stress-ratio factor was reported in reference 4, where it is shown to be an improved method for comparing air-cooled blades.

Verification of Simple Criteria for Three Coolant Passage

Configurations of Profile 1

Analysis by simple criteria. - To verify the simple criteria proposed herein for the evaluation of turbine blades, the two blades for which experimental data had previously been obtained were evaluated first. In addition, a coolant passage that was believed to be better was also evaluated. The simple criteria for the three coolant passage configurations for the turbine rotor blade of the centrifugal-flow-compressor turbojet engine are compared in table I. Because of the high tip speeds and the relatively small diameter of the centrifugal-flow-compressor engine, the blade shell was tapered from 0.020 inch at the blade tip to 0.060 inch at the blade root to obtain reasonable blade stresses. The values presented in the table were obtained from cross-sectional layouts which were ten times the size of the actual configurations, and in all cases the small fillets formed by the braze material were neglected. Higher values of all the simple criteria, with the exception of the weight criterion, indicate the more desirable blades.

Configuration A: This blade with 10 tubes in the coolant passage has been proved (reference 4) to be satisfactory and therefore the values of the cooling effectiveness criterion, weight criterion, stress criterion, and pressure-loss criterion (see table I) were taken as base values with which other configurations were compared.

Configuration B: This blade, in which the cooling air is forced to flow between the insert and the blade shell and in which the heat is dissipated by means of the small fins, should require less cooling-air flow than configuration A to maintain a given blade temperature, since the value of the cooling effectiveness criterion was larger. Configuration B was some 22 percent heavier than configuration A as shown by the weight criterion. The stress criterion indicated that configuration B would have a higher centrifugal stress at the blade root than configuration A and, because of the smaller hydraulic diameter of configuration B, its pressure loss would be greater.

Configuration C: It was thought that blades with relatively thin profiles should not need inserts because the internal surfaces or fins would be short enough that they would be effective even near the mean camber line of the blade. Therefore fins made from 0.010 inch sheet metal in the form of corrugations were placed entirely across the blade. Although the total volume of metal in the airfoil is somewhat larger than that in configuration A, the cooling effectiveness criterion is larger, indicating that less cooling air would be required. The stress criterion indicates a higher centrifugal stress at the blade root than that of either of the other configurations and the smaller hydraulic diameter implies a larger pressure loss.

Since the weight and pressure-loss criteria of configuration C do not vary considerably from those of configuration B, blade C would probably be chosen as the best blade because of its high cooling effectiveness. The choice of configuration C over configuration B would, however, be influenced by the relative complexity of the required fabrication techniques.

Analysis by detailed analytical methods. - To check the results obtained for the three coolant passage configurations of profile 1 by means of the simple criteria, the cooling effectiveness, stress-ratio factors, and pressure losses were evaluated using the detailed analytical equations.

Cooling effectiveness: The variation of average blade temperature at a position $l\frac{7}{16}$ inches from the blade root with cooling-air flow ratio is shown in figure 7 for the three internal passage configurations of profile 1. The cooling-air inlet temperature at the blade root was assumed to be 180° F. For a given average blade temperature in the range from 900° to 1100° F, the tube-filled blade, configuration A, requires 55 to 80 percent more cooling air than does configuration C.

Figure 7 also verifies the trends predicted by the cooling effectiveness criteria of table I. To maintain a certain blade temperature, configuration A would require the largest amount of cooling air and configuration C, the smallest.

Stresses and stress-ratio factor: The stress criterion at the blade root $A_{\text{tap}}/A_{\text{untap}}$ as presented in table I was verified by detailed analytical calculations of the centrifugal stresses. The relative differences among the centrifugal stresses at the blade root for the three configurations, however, were not so great as would be expected from the simple criteria. The large differences among the simple criteria for the

three configurations existed because A_{tap} was quite large compared with A_{untap} ; small variations in A_{untap} resulted in the large differences between the ratios. A comparison of the actual stress and the simple criterion is given in the following table:

Configuration	Stress criterion $\frac{A_{tap}}{A_{untap}}$	Centrifugal stress at blade root (psi)
A	5.24	32,600
B	4.26	33,150
C	3.90	33,400

A comparison of the three internal passage configurations is shown in figure 8 on the basis of stress-ratio factor and cooling-air flow ratio. With a stress-ratio factor of 2.0, configuration A would require a cooling-air flow ratio of approximately 0.012, configuration B would require a cooling-air flow ratio near 0.009, and configuration C would require a cooling-air flow ratio of 0.0075; that is, the cooling-air flow ratio for configuration B would be approximately 25 percent less than that required for configuration A, and that for configuration C would be about 37 percent less than that for configuration A. This comparison, on the basis of stress-ratio factor and cooling-air flow ratio, also substantiates the relative cooling effectiveness shown in table I. Thus the analysis indicates that if a stress-ratio factor of around 2.0 is adequate (reference 4), both finned configurations (B and C) for the high-stress turbine for the centrifugal-flow-compressor turbojet engine should operate at sea-level static engine conditions at cooling-air flow ratios below 0.01. It should be remembered, however, that the simple stress criterion A_{tap}/A_{untap} is an indication of only the blade centrifugal stress and does not necessarily select the blade with the best stress-ratio factor since the stress-ratio factor is also very dependent on the blade cooling effectiveness.

Pressure losses: The use of the hydraulic diameter as an indication of the relative pressure losses, assuming a constant cooling-air flow rate, was verified. (As the hydraulic diameter increased the pressure losses decreased.) Equations (10) and (11) were used and the static cooling-air pressure at the blade tip was assumed to be 23.75 pounds per square inch absolute. The results of the detailed calculations, both for a constant cooling-air weight flow to verify the pressure loss criteria and for a constant stress-ratio factor of 2.0, are shown in the following table. It should be noted that pressure rises were obtained for all three configurations and an increased pressure rise

indicates a decreased pressure loss. Thus, for the three configurations considered, the hydraulic diameter will increase as the pressure rise increases. Pressure rises were obtained because the Mach numbers in the cooling-air passages were quite low and the pumping action of the blades was greater than the inherent pressure drop through the blade.

Configuration	Pressure-loss criterion \bar{D}_h (in.)	Pressure loss through blade $P_{a,T} - P_{a,h}$ (lb/sq in.)	
		Coolant flow constant at 0.0162 lb/sec	Stress-ratio factor constant at 2.0
A	0.0759	5.44	5.44
B	.0576	4.75	5.13
C	.0506	4.70	5.09

In conclusion, the method which involves the simple criteria gives an accurate relative evaluation of the three coolant passage configurations of the turbine blade for the centrifugal-flow-compressor engine.

Illustration of Selection of Coolant Passage Configuration

for Profile 2

Analysis by simple criteria. - As a further example of the application of the simple criteria, a coolant passage configuration was selected for the turbine rotor blade of an engine with an axial-flow compressor. Nine coolant passage configurations were considered. In table II are presented the values of the criteria considered for the various configurations, the metal thicknesses of the component parts, and a sketch of each configuration. The blade shell was 0.018 inch thick with no taper. Since this blade has no taper, the centrifugal stress at the blade root was the same for all configurations considered and the value of the stress criterion was zero. The blades are presented in the order in which they were considered. The values presented in the table were obtained from ten times the actual size layouts. Here again, the effect of the braze material was neglected.

Configuration A: The first configuration considered was a tube-filled blade in which the blade shell was packed with 23 small tubes (see table II for tube sizes). Although the cooling effectiveness

criteria appeared to be reasonable, the total volume of metal in the airfoil section was large and it was thought a lighter configuration could be found. Also, the coolant flow area was much larger than that of blades previously investigated (profile 1) and it was considered advantageous to reduce this area in an effort to increase the inside heat-transfer coefficient. The pressure loss criterion \bar{D}_h was of the same order of magnitude as that of profile 1.

Configuration B: This configuration is the same as configuration A except that the tubes in the center of the pack have been blocked off by means of a cap at the base of the blade. It was realized that this blade would be heavier than configuration A, but it was considered in order to examine the effect of this blockage on the cooling effectiveness criterion. This criterion was found to change very little, although the cooling-air flow area was considerably smaller. The pressure-loss criterion was also smaller, indicating a slightly larger pressure loss.

Configuration C: In an effort to utilize sheet metal instead of tubes to form the internal heat-transfer surface and reduce the weight of the blade, configuration C was evolved. This blade was about 30 percent lighter than the first two configurations considered, but the cooling effectiveness criterion was quite small. It was also thought that the points of contact between the internal surfaces and the blade shell were spaced too far apart. With the thin blade shell (0.018 inch) and the wide spacing, large temperature gradients would probably occur in the blade shell between the points of contact. The hydraulic diameter, however, was quite large and therefore the pressure losses would be low.

Configuration D: This configuration was made in an effort to increase the cooling effectiveness criterion over that obtained in configuration C by increasing the amount of cooled surface area. The metal thickness of the corrugations was double that used for configuration C to keep the coolant flow area small. Although the cooled surface area increased considerably, the coolant flow area also increased and the resulting cooling effectiveness criterion was still considered too small. The volume of metal in the airfoil section was approaching the values of configurations A and B, which were considered too heavy. The pressure loss criterion, however, was larger than the criteria of configurations A and B.

Configuration E: It was decided that blades which are quite thick in the midchord region, such as profile 2, should have an insert in the center of the blade so that the cooling air is forced to flow in an annulus next to the blade shell where it would be most effective. Such an insert was provided in configuration E. Here the corrugations were

0.015 inch in thickness and the cooling effectiveness criterion was larger than the criteria of configurations C and D, but not so large as those of A and B. The blade weight, however, was approximately 15 percent lower than the weights of configurations A and B. The pressure-loss criterion was smaller than the criteria of C and D, but larger than those of A and B. Here again it was thought that the points of contact of the internal corrugations and the blade shell were too far apart.

Configuration F: This configuration was made in an attempt to obtain a high value of the cooling effectiveness criterion by the use of a large insert. This was accomplished and the volume of metal in the airfoil section was lower than any previously considered with the exception of that of configuration C. This configuration was discarded, however, because the nonuniformity of the corrugations did not appear desirable with regard to fabrication and it was quite probable that some of the very small passages in the midchord region would become plugged when the assembly was brazed. Also, these small passages in the midchord region would have a higher pressure drop than the passages in the leading- and trailing-edge sections, and it is possible that the midchord passages would receive little cooling air. This configuration had the smallest hydraulic diameter of the coolant passage configurations considered.

Configuration G: With 0.015 inch thick sheet metal for the corrugations, this configuration had a cooling effectiveness criterion comparable with the criteria of configurations A and B, but was only about 7.5 percent less in weight. Also, the corrugations were not uniform.

Configuration H: This blade is quite similar to configuration G with the exceptions that uniform corrugations were used and 0.010 inch thick sheet metal was used for the insert and corrugations. The resulting blade has a value of cooling effectiveness criterion approximately the same as that of configuration G and the coolant flow area was considered reasonable. The total volume of metal in the airfoil section was approximately 25 percent lower than in configuration A. The pressure-loss criterion appeared adequate when compared with the values obtained for the other configurations. The pitch of the corrugations was such that large temperature gradients in the shell would not be encountered as the heat was conducted from the shell into the corrugations. This configuration appeared desirable on the basis of comparison of the various criteria and required fabrication procedures and was selected for a more thorough analysis to determine the required cooling-air flow ratios, required cooling-air pressure at the blade base, and the variation of the stress-ratio factor with cooling-air flow ratio.

Configuration I: Although it was thought that this configuration would probably be heavier than configuration H, the sheet metal corrugations were simulated by utilizing tubes placed around the insert. Configuration I was approximately 20 percent heavier than configuration H, but the cooling effectiveness criterion was larger, indicating better cooling effectiveness. This is somewhat misleading in that the braze material was neglected. A large portion of the cooled surface area is obtained by the small passages between the tubes and it is quite probable that a large number of these passages would become plugged when the blade assembly is brazed together. On the assumption that these passages would remain open, the effective inside heat-transfer coefficient \bar{h}_f was determined and compared with that obtained for configuration H.

Analysis by detailed methods. - Detailed analytical calculations were made on configurations H and I, insert blades with fins and tubes, respectively, of profile 2 for a comparison of the average effective inside heat-transfer coefficients. Further calculations were made for configuration H to determine the absolute values of the cooling effectiveness, stress-ratio factor, and pressure losses.

Cooling effectiveness: The first comparison made (fig. 9) was the relation of the average effective inside heat-transfer coefficient \bar{h}_f to the inside heat-transfer coefficient $\bar{h}_{a,B}$ for configurations H and I, the two best configurations of profile 2 as determined on the basis of the simple criteria. Over a range of anticipated cooling-air weight flows (0.015 to 0.040 lb/sec) the average inside heat-transfer coefficient $\bar{h}_{a,B}$ of configuration H was found to be approximately 5 percent lower than that obtained for configuration I and the coefficients were in the range of 0.01 (Btu/(sec)(sq ft)(°F)). Figure 9 shows that there was a significant difference between the effective coefficients only at the higher values of the inside heat-transfer coefficient $\bar{h}_{a,B}$. However, the facts that for the same cooling-air weight flow configuration I has a higher average inside heat-transfer coefficient $\bar{h}_{a,B}$ and that for the same values of $\bar{h}_{a,B}$ configuration I has a higher \bar{h}_f bear out the results of the simple analysis wherein it was shown that the cooling effectiveness criterion was larger for configuration I than for configuration H. The difference in the region of 0.01 (Btu/(sec)(sq ft)(°F)) between the average effective inside heat-transfer coefficients \bar{h}_f of configurations H and I was not sufficient to warrant any further consideration of configuration I, since, as pointed out in the previous section, configuration I has the disadvantage of being heavier than configuration H. It was also thought that this small difference in the average effective inside heat-transfer coefficient would undoubtedly be eliminated by closing a few of the small passages between the tubes of configuration I when brazing

the component parts of the blade. The low heat-transfer coefficient was due to the large cooling-air flow area and the over-all cooling effectiveness of these two configurations could be increased by increasing the inside heat-transfer coefficient.

Figure 10 shows for configuration H the variation of the average analytical blade-shell temperature at a position 1.5 inches from the blade root with cooling-air flow ratio for a cooling-air inlet temperature of 180° F. The values used in this analysis are given in table III. This figure was obtained by solving equation (1) for the average blade temperatures over a range of cooling-air weight flow. The critical blade section, or the span position where a blade radial temperature curve was tangent to the blade shell temperature-distribution curve (see fig. 1) was found to be 1.5 inches from the blade root. The use of a cooling-air inlet temperature of 180° F assumed that the cooling air is obtained from one of the earlier stages of the compressor or that it is cooled by means of a heat exchanger or expansion system before it reaches the blade. At cooling-air flow ratios of 0.01 to 0.02, the average blade temperatures varied from 1150° to 1035° F.

Stresses and stress-ratio factor: Because of the conservative centrifugal stresses in the turbine of the axial-flow-compressor turbojet engine, a nontapered rotor blade shell could be utilized. The centrifugal stress at the root of the rotor blade for the conditions investigated was 28,000 pounds per square inch.

In figure 11 the stress-ratio factor, the ratio of the allowable stress to the actual centrifugal stress, is plotted against the cooling-air flow ratio. If the stress-ratio factor of 2.0 is assumed adequate (reference 4), the required cooling-air flow ratio for a cooling-air inlet temperature of 180° F is 0.013 when the blade material is assumed to be Timken alloy 17-22A(S).

Pressure losses: The required cooling-air static pressure at the blade root was determined from the required cooling-air flow ratio for a stress-ratio factor of 2.0. A static pressure at the blade tip of 31.5 pounds per square inch absolute and equations (10) and (11) were used to find the required static pressure at the blade root, which was 26.4 pounds per square inch absolute. This pressure rise in the blade indicates that the compressor can probably be bled at some stage before the compressor discharge at sea-level static engine conditions. With the pressure required for bleed at the compressor assumed as 35.0 pounds per square inch absolute (this allowed over 8.0 pounds per square inch pressure loss from the compressor to the base of the blade), the cooling-air temperature was slightly higher than 180° F, but the change in required coolant flow ratio was negligible.

Comparison of Profiles 1 and 2

All the internal passage configurations considered herein can be assumed to be a form of fin. It is known that for a given fin thickness there is a finite length of fin that can be utilized effectively, and beyond this length little additional effective heat-transfer surface area can be gained. Therefore, in blades similar to profile 2 which is quite thick in the midchord region, the analysis indicated that an insert should be used. This allows the use of shorter fins; also, the cooling air is directed near the heated surfaces of the blade shell and higher inside heat-transfer coefficients can be obtained for a given amount of cooling air because the use of the insert decreases the coolant flow area. In axial-flow-compressor engines of moderate tip speeds, it is possible to utilize nontapered blade shells and not exceed reasonable values of stress at the blade root. The use of nontapered shells reduces the blade weight and, as a consequence, lighter disks can be employed.

Blades with thin profiles, such as that described herein for the centrifugal-flow-compressor turbojet engine, do not appear to require inserts. In fact, it was found that the most effective configuration was obtained by using thin corrugations across the entire blade width. The higher tip speeds of the centrifugal-flow-compressor engine necessitated the use of a tapered blade shell to withstand the centrifugal loads and the blade weight, due in part to this tapered shell, was approximately the same as that of the larger chord blade for the axial-flow-compressor engine.

For both profiles considered, the simple criteria proposed herein provided an excellent screening method for evaluating a number of configurations and, by using such a design method, it was possible to evolve blades that required low coolant flow rates. In both cases the pressure losses were quite low, in fact, the pumping action due to rotation was higher than the pressure loss due to friction so that there was an actual pressure rise.

SUMMARY OF RESULTS

The results of an investigation wherein a method based on geometric factors of the coolant passage was evolved for the rapid selection and evaluation of coolant passage configurations for air-cooled turbine rotor blades are summarized as follows:

1. The analytical average blade temperatures and stress-ratio factors based on analytical temperatures at a span position of $1\frac{7}{16}$ inches, approximately 1/3-span position, from the blade root for two coolant passage configurations for the blade for the engine with a centrifugal-flow compressor showed good agreement with the experimental average blade temperatures and stress-ratio factors based on experimental temperatures. In both cases the analytical blade temperatures were 40° to 60° F lower than the experimental temperatures.
2. The simple criteria evolved for the selection and relative evaluation of a coolant passage configuration were: (1) the ratio of the internal cooled surface area to the 1.2 power to the coolant flow area for the heat-transfer or cooling effectiveness criterion; (2) the ratio of the cross-sectional metal area of the tapered member of the blade to the area of the untapered members for the strength criterion; (3) the volume of metal in the blade shell for the weight criterion; and (4) the hydraulic diameter for the pressure-loss criterion.
3. The method which involves the simple criteria was found to give an accurate relative evaluation of the three coolant passage configurations of the turbine blade for the centrifugal-flow-compressor turbojet engine.
4. By the use of this blade evaluation method, a coolant passage configuration with a high cooling effectiveness, an insert blade with fins, was selected for the turbine of the axial-flow-compressor turbojet engine. The detailed analytical equations were used to show that for a stress-ratio factor of 2.0 and a cooling-air inlet temperature of 180° F, this blade would require a cooling-air flow ratio of 0.013.
5. At a stress-ratio factor of 2.0 for the three configurations for the turbine of the centrifugal-flow-compressor engine and the insert blade with fins for the axial-flow-compressor engine, it was found that there was a static pressure rise through the coolant passages. Because of the high cooling effectiveness and therefore low cooling-air requirements for these four configurations, the cooling-air Mach numbers in the passages were quite low and the pumping action of the blades was greater than the inherent pressure drop through the blade.

Lewis Flight Propulsion Laboratory
National Advisory Committee for Aeronautics
Cleveland, Ohio

APPENDIX A

SYMBOLS

The following symbols are used in this report:

- A flow area, sq ft or sq in.
- A_{tap} metal cross-sectional area of tapered member of blade, sq ft or sq in.
- A_{untap} metal cross-sectional area of untapered members of blade, sq ft or sq in.
- b blade length or span, ft or in.
- c_p specific heat at constant pressure, Btu/(lb)(°F)
- D_h hydraulic diameter, $\frac{4 \text{ times flow area}}{\text{wetted perimeter}}$, ft or in.
- Eu Euler number
- \bar{F} mean coefficient, $\frac{\bar{Nu}_{g,B}}{\left(\bar{Re}_{g,B}\right)^2 \left(\bar{Pr}_{g,B}\right)^{\frac{1}{3}}}$
- f friction coefficient
- g standard acceleration of gravity, ft/sec²
- h convection heat-transfer coefficient, Btu/(sec)(sq ft)(°F)
- \bar{h}_f average effective inside heat-transfer coefficient, Btu/(sec)(sq ft)(°F)
- K, K', K'', K''' constants
- k thermal conductivity, Btu/(sec)(ft)(°F)
- L effective fin length, ft or in.
- l perimeter, ft or in.
- l_w total wetted perimeter, ft or in.

- M Mach number relative to blade
- m fin spacing, ft or in.
- N engine speed, rpm
- $\overline{Nu}_{g,B}$ mean Nusselt number based on perimeter divided by π , $\frac{\overline{h}_o l_o}{\pi \overline{k}_{g,B}}$
- n number of sections of equivalent fins
- $\overline{Pr}_{g,B}$ mean Prandtl number, $\frac{\overline{c}_{p,g,B} \overline{\mu}_{g,B}}{\overline{k}_{g,B}}$
- p static pressure, lb/(sq ft) absolute
- Q heat added to cooling air, Btu/sec
- R gas constant, ft-lb/(lb)(°R)
- $\overline{Re}_{g,B}$ mean Reynolds number based on perimeter divided by π ,

$$\frac{\rho_{g,B} W l_o}{\pi \overline{\mu}_{g,B}}$$
- $\overline{Re}_{a,B}$ mean inside Reynolds number based on hydraulic diameter,

$$\frac{w_a \overline{D}_h}{\overline{A}_a \overline{\mu}_{a,B}} \cdot \frac{\overline{T}'_a}{\overline{T}_B}$$
- r distance from turbine center line to any point on turbine blade, ft or in.
- S heat-transfer surface area, sq ft or sq in.
- T static temperature, °F or °R
- T' total temperature, °F or °R
- W relative velocity, ft/sec
- w weight flow, lb/sec
- x spanwise distance from blade root to any point on blade, ft or in.

z	exponent of Reynolds number, equation (2)
α	number of fins in particular section of blade
β	exponent
γ	ratio of specific heats
θ	exponent
λ	$\frac{\bar{h}_o l_o}{\bar{h}_f l_i}$
μ	absolute viscosity, lb/(ft)(sec)
ξ	transition ratio
ρ	density, lb/cu ft
τ	fin thickness, ft or in.
φ	$\sqrt{\frac{2 \bar{h}_{a,B}}{\tau k_B}}$
φ_ω	rotational correction parameter (see reference 12)
ψ	rotational correction parameter (see reference 12)
ω	angular velocity, radians/sec

Subscripts:

a	cooling air
B	blade (When used with fluid properties or in heat-transfer equations, subscript B indicates "based on average blade temperature at critical section.")
e	effective
g	combustion gas
h	blade root

- i inside
- ζ index summation
- m mean value (see equation (11))
- o outside
- T blade tip
- t used with T_B to denote temperature of total (or wetted)
 heat-transfer surface and with S_i to denote total inside
 heat-transfer surface
- 1,2 blade sections (see figs. 12 and 13)
- A,A',B, designate end points of inside perimeter of section of equiva-
B',C,C' lent fins (see figs. 12 and 13)

The bar indicates average or mean value.

APPENDIX B

SAMPLE CALCULATIONS FOR DETERMINING \bar{h}_f FOR CORRUGATED
AND TUBED BLADES

An average effective inside heat-transfer coefficient \bar{h}_f is calculated for a typical corrugated blade (configuration B, profile 1) using equations (6) through (9). The same procedure is applied to a typical tubed blade (configuration A, profile 1) but the intermediate steps involving numerical calculations are omitted. The main difference between configurations B and A in the determination of a relation between \bar{h}_f and $\bar{h}_{a,B}$ is the selection of equivalent fin sections. Since the selection of equivalent fin sections for a corrugated-type blade is relatively simple, configuration B will be considered first.

By inspection, configuration B is divided into two equivalent fin sections which appear to have equal length fins, and the number of fins in each section is determined (see fig. 12). Section 1 includes the midchord region of the blade between AA' and BB', and section 2 includes both the leading- and trailing-edge regions ACB and A'C'B' (see fig. 12(a)). The following quantities were determined from a 10 times size drawing of configuration B, or calculated from equation (7), (8), or (9):

Section 1

Number of fins, α_1	26
Inside blade shell perimeter, $l_{i,1} = l_{i,AA'} + l_{i,BB'}$, in.	2.040
ft	0.1699
Total wetted perimeter, $l_{W,1}$, in.	7.496
ft	0.6247
Fin thickness, τ_1 , in.	0.010
ft	0.000833
Corrugation conductivity, $k_{B,1}$, Btu/(sec)(ft)(°F)	0.00708

Section 2

Number of fins, α_2	12
Inside blade shell perimeter, $l_{i,2} = l_{i,ACB} + l_{i,A'C'B'}$, in.	1.644
ft	0.1370
Total wetted perimeter, $l_{W,2}$, in.	3.124
ft	0.2603
Fin thickness, τ_2 , in.	0.010
ft	0.000833
Corrugation conductivity, $k_{B,2}$, Btu/(sec)(ft)(°F)	0.00708

Since $\tau_1 = \tau_2$ and $k_{B,1} = k_{B,2}$, then $\varphi_1 = \varphi_2$; thus

$$\varphi_1 = \varphi_2 = \sqrt{\frac{2 \bar{h}_{a,B}}{\tau k_B}} = \sqrt{\frac{2 \bar{h}_{a,B}}{(0.00708)(0.000833)}}$$

Now $\alpha_\xi m_\xi$ and L_ξ will be determined for sections 1 and 2 from equations (8) and (9) giving

$$\alpha_1 m_1 = 0.1483 \text{ foot} \quad L_1 = 0.00917 \text{ foot}$$

$$\alpha_2 m_2 = 0.1270 \text{ foot} \quad L_2 = 0.00556 \text{ foot}$$

Writing equation (6) for configuration B gives

$$\bar{h}_f = \frac{\bar{h}_{a,B}}{\sum_{\xi=1}^{n=2} \alpha_\xi (m_\xi + \tau_\xi)} \left[\sum_{\xi=1}^{n=2} \frac{\alpha_\xi (2L_\xi) \tanh(L_\xi \varphi_\xi)}{L_\xi \varphi_\xi} + \sum_{\xi=1}^{n=2} \alpha_\xi m_\xi \right] \quad (B1)$$

or

$$\bar{h}_f = \frac{\bar{h}_{a,B}}{l_{i,1} + l_{i,2}} \left[\frac{\alpha_1 (2L_1) \tanh(L_1 \varphi_1)}{L_1 \varphi_1} + \frac{\alpha_2 (2L_2) \tanh(L_2 \varphi_2)}{L_2 \varphi_2} + (\alpha_1 m_1 + \alpha_2 m_2) \right] \quad (B2)$$

Substituting the indicated values in equation (B2) results in

$$\bar{h}_f = \bar{h}_{a,B} \left[0.896 + 1.554 \frac{\tanh(5.339 \sqrt{\bar{h}_{a,B}})}{(5.339 \sqrt{\bar{h}_{a,B}})} + 0.433 \frac{\tanh(3.237 \sqrt{\bar{h}_{a,B}})}{(3.237 \sqrt{\bar{h}_{a,B}})} \right] \quad (B3)$$

Thus, by assuming values of $\bar{h}_{a,B}$, a curve similar to the curves shown in figure 9 is obtained.

For a tubed blade such as configuration A, profile 1, equivalent fin sections are not so obvious as for a corrugated type blade and the following procedure is suggested: Determine the equivalent fin sections by assuming points of zero temperature gradient. For example, configuration A is divided into two equivalent fin sections which appear to have equal length fins (see fig. 13). Section 1 includes the leading- and trailing-edge regions of the blade ACB and A'C'B', and section 2 includes the midchord region of the blade between AA' and BB' (see fig. 13(a)). This fin division is based on the assumption that the temperature gradient is zero between tubes at tube junctions and thus the tubes are essentially considered as not being interconnected. Also, the temperature gradient is zero at points of symmetry (see fig. 13(b)). Therefore the two tubes nearest the leading- and trailing-edge regions constitute one equivalent fin section (section 1) containing eight fins. Section 2 consists of the remaining eight tubes, each of which is attached to only one wall, and contains 16 fins. Once the equivalent fin sections were determined for configuration A, the necessary measurements were obtained and the following relation resulted:

$$\bar{h}_f = \bar{h}_{a,B} \left[0.879 + 2.282 \frac{\tanh \left(7.675 \sqrt{\bar{h}_{a,B}} \right)}{\left(7.675 \sqrt{\bar{h}_{a,B}} \right)} + 0.571 \frac{\tanh \left(3.84 \sqrt{\bar{h}_{a,B}} \right)}{\left(3.84 \sqrt{\bar{h}_{a,B}} \right)} \right]$$

REFERENCES

1. Ellerbrock, Herman H., Jr., and Stepka, Francis S.: Experimental Investigation of Air-Cooled Blades in Turbojet Engine. I - Rotor Blades with 10 Tubes in Cooling-Air Passages. NACA RM E50I04, 1950.
2. Hickel, Robert O., and Ellerbrock, Herman H., Jr.: Experimental Investigation of Air-Cooled Turbine Blades in Turbojet Engine. II - Rotor Blades with 15 Fins in Cooling-Air Passages. NACA RM E50I14, 1950.
3. Stepka, Francis S., and Hickel, Robert O.: Experimental Investigation of Air-Cooled Turbine Blades in Turbojet Engine. IX - Evaluation of the Durability of Noncritical Rotor Blades in Engine Operation. NACA RM E51J10, 1951.
4. Esgar, Jack B., and Clure, John L.: Experimental Investigation of Air-Cooled Turbine Blades in Turbojet Engine. X - Endurance Evaluation of Several Tube-Filled Rotor Blades. NACA RM E52B13, 1952.
5. Bartoo, Edward R., and Clure, John L.: Experimental Investigation of Air-Cooled Turbine Blades in Turbojet Engine. XII - Cooling Effectiveness of a Blade with an Insert and with Fins Made of a Continuous Corrugated Sheet. NACA RM E52F24.

6. Long, Roger A., and Esgar, Jack B.: Experimental Investigation of Air-Cooled Turbine Blades in Turbojet Engine. VII - Rotor-Blade Fabrication Procedures. NACA RM E51E23, 1951.
7. Livingood, John N. B., and Brown, W. Byron: Analysis of Spanwise Temperature Distribution in Three Types of Air-Cooled Turbine Blade. NACA Rep. 994, 1950. (Supersedes NACA RM's E7B11e and E7G30.)
8. Livingood, John N. B., and Brown, W. Byron: Analysis of Temperature Distribution in Liquid-Cooled Turbine Blades. NACA TN 2321, 1951.
9. Freche, John C., and Schum, Eugene F.: Determination of Blade-to-Coolant Heat-Transfer Coefficients on a Forced-Convection, Water-Cooled, Single-Stage Turbine. NACA RM E51E18, 1951.
10. Schum, Eugene F., Freche, John C., and Stelpflug, William J.: Comparison of Calculated and Experimental Temperatures of Water-Cooled Turbine Blades. NACA RM E52D21, 1952.
11. Brown, W. Byron, and Rossbach, Richard J.: Numerical Solution of Equations for One-Dimensional Gas Flow in Rotating Coolant Passages. NACA RM E50E04, 1950.
12. Brown, W. Byron, and Slone, Henry O.: Pressure Drop in Coolant Passages of Two Air-Cooled Turbine-Blade Configurations. NACA RM E52D01, 1952.
13. Ellerbrock, Herman H., Jr., and Ziemer, Robert R.: Preliminary Analysis of Problem of Determining Experimental Performance of Air-Cooled Turbine. I - Methods for Determining Heat-Transfer Characteristics. NACA RM E50A05, 1950.
14. Esgar, Jack B., and Lea, Alfred L.: Determination and Use of the Local Recovery Factor for Calculating the Effective Gas Temperature for Turbine Blades. NACA RM E51G10, 1951.
15. Brown, W. Bryon, and Donoughe, Patrick L.: Extension of Boundary-Layer Heat-Transfer Theory to Cooled Turbine Blades. NACA RM E50F02, 1950.
16. Hubbartt, James E., and Schum, Eugene F.: Average Outside-Surface Heat-Transfer Coefficients and Velocity Distributions for Heated and Cooled Impulse Turbine Blades in Static Cascades. NACA RM E50L20, 1951.

17. Humble, Leroy V., Lowdermilk, Warren H., and Desmon, Leland G.:
Measurements of Average Heat-Transfer and Friction Coefficients for
Subsonic Flow of Air in Smooth Tubes at High Surface and Fluid
Temperatures. NACA Rep. 1020, 1951. (Supersedes NACA RM's E7L31,
E8L03, E50E23, and E50H23.)
18. Slivka, William R., and Silvern, David H.: Analytical Evaluation of
Aerodynamic Characteristics of Turbines with Nontwisted Rotor Blades.
NACA TN 2365, 1951.
19. Heaton, Thomas R., Slivka, William R., and Westra, Leonard F.: Cold-
Air Investigation of a Turbine with Nontwisted Rotor Blades Suitable
for Air Cooling. NACA RM E52A25, 1952.

TABLE I - COMPARISON OF SIMPLE CRITERIA BASED ON GEOMETRIC FACTORS FOR THREE COOLANT PASSAGE CONFIGURATIONS FOR AIR-COOLED ROTOR BLADE OF PROFILE 1



[Braze material neglected; airfoil length, 4 in.; shell thickness, 0.060 in. at blade root and 0.020 in. at blade tip; area of heated surface, 15.70 sq in.]




Configuration	Metal thickness of corrugation or tube size (in.)			Metal thickness of insert (in.)	Metal thickness of cap (in.)	Cooled surface area $S_{i,t}$ (sq in.)	Coolant flow area \bar{A}_a (sq in.)	Cooling effectiveness criterion $\frac{S_{i,t}^{1.2}}{\bar{A}_a}$	Weight criterion, total volume of metal in airfoil (cu in.)	Stress criterion $\frac{A_{tap}}{A_{untap}}$	Pressure-loss criterion \bar{D}_h (in.)
	Number of tubes	Out-side diam.	Wall thickness								
A 	10	0.125	0.0125	-----	-----	40.60	0.193	441	0.786	5.24	0.0759
B 	0.010			0.010	0.030	42.48	0.153	587	0.826	4.26	0.0576
C 	0.010			-----	-----	53.92	0.171	698	0.847	3.90	0.0506

TABLE II - COMPARISON OF SIMPLE CRITERIA BASED ON GEOMETRIC FACTORS FOR NINE COOLANT PASSAGE CONFIGURATIONS FOR AIR-COOLED ROTOR BLADE OF PROFILE 2

[Braze material neglected; airfoil length, 3.70 in.; shell thickness, 0.018 in.; area of heated surface, 20.13 sq in.]








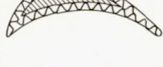

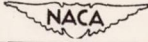
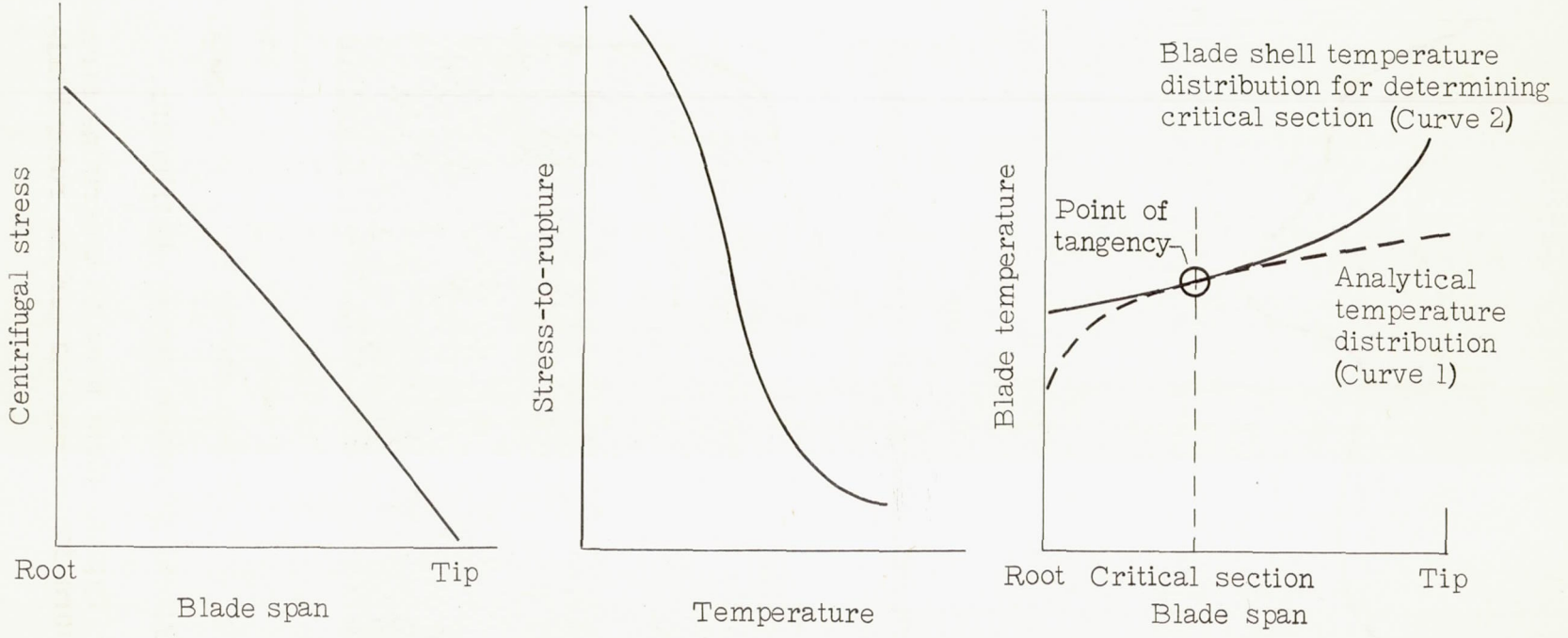
Configuration	Metal thickness of corrugation or tube size (in.)			Metal thickness of insert (in.)	Metal thickness of cap (in.)	Cooled surface area $S_{1,t}$ (sq in.)	Coolant flow area \bar{A}_a (sq in.)	Cooling effectiveness criterion $\frac{S_{1,t}^{1.2}}{\bar{A}_a}$	Weight criterion, total volume of metal in airfoil (cu in.)	Stress criterion $\frac{A_{tap}}{A_{untap}}$	Pressure-loss criterion $\frac{D_h}{D_h}$ (in.)
	Number of tubes	Out-side diam.	Wall thickness								
	5	0.190	0.02	-----	----	85.83	0.416	500	1.041	0	0.0717
	13	.156	.02								
	5	.125	.0125								
	5	0.190	0.02	-----	0.03	66.88	0.303	508	1.044	0	0.0670
	13	.156	.02								
	5	.125	.0125								
	0.01			-----	0.02	46.50	0.395	253	0.704	0	0.1257
	0.02			-----	----	75.00	0.541	329	0.945	0	0.1067
	0.015			0.015	0.03	69.18	0.411	394	0.877	0	0.0880
	0.015			0.015	0.03	63.97	0.251	582	0.846	0	0.0581
	0.015			0.015	0.03	77.89	0.386	482	0.964	0	0.0734
	0.01			0.01	0.03	78.04	0.396	472	0.783	0	0.0750
	1	0.190	0.02	0.01	0.03	93.20	0.396	583	0.966	0	0.0628
	1	.156	.02								
	26	.125	.0125								

TABLE III - CONDITIONS DETERMINING COOLING REQUIREMENTS



Item	Profile 1			Profile 2
	Configuration			Configuration
	A	B	C	H
Compressor weight flow, w_g , lb/sec	74.10	74.10	74.10	94.00
Effective gas temperature, $T_{g,e}$, °F	1446	1446	1446	1391
Engine speed, rpm	11,500	11,500	11,500	7900
Effective cooling-air temperature at blade root, $T_{a,e,h}$, °F	180	180	180	180
Number of rotor blades	54	54	54	72
Rotor blade span, b , in.	4.00	4.00	4.00	3.70
Outside blade perimeter, l_o , in.	3.93	3.93	3.93	5.44
Rotor blade chord (axial), in.	1.76	1.76	1.76	2.27
Average outside heat-transfer coefficient, \bar{h}_o , Btu/(sec)(sq ft)(°F)	0.0548	0.0548	0.0548	0.0558



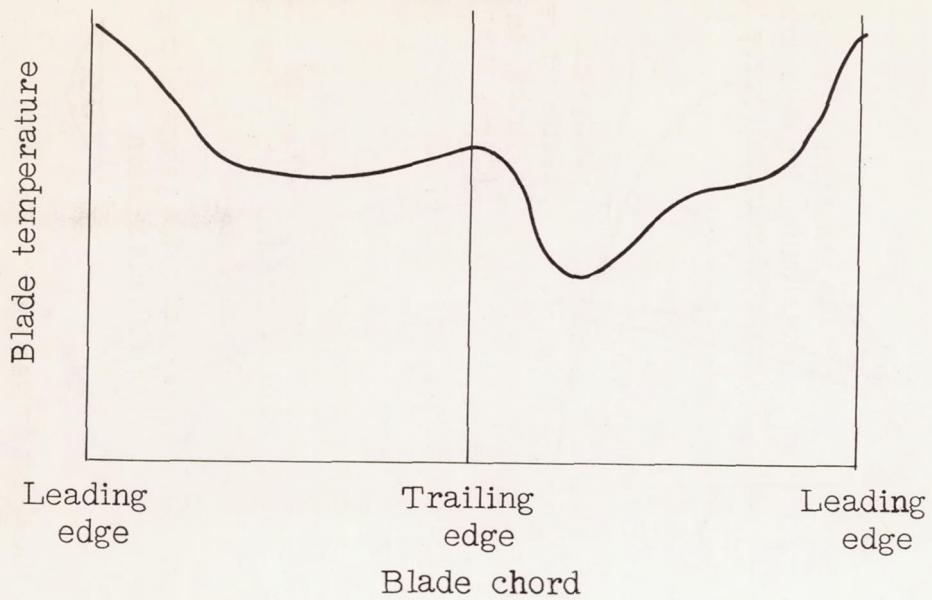
(a) Variation of blade centrifugal stress with blade span.

(b) Variation of stress-to-rupture with temperature for 100-hour life of typical noncritical steel.

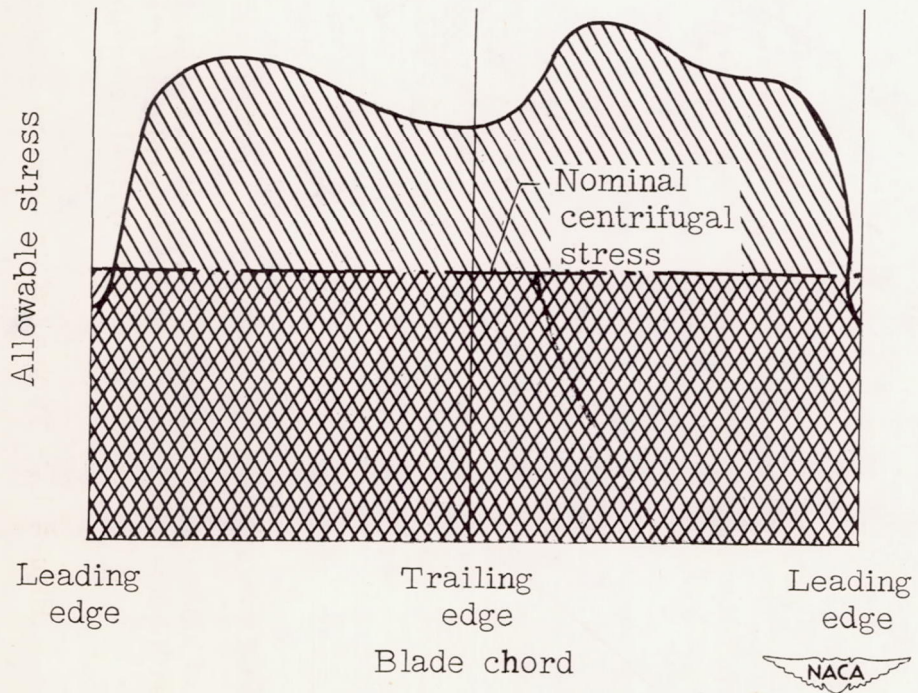
(c) Variation of blade temperature with blade span.



Figure 1. - Typical plots used to determine critical blade section.

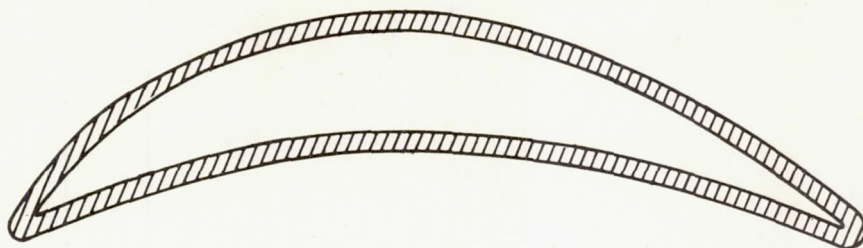


(a) Typical blade temperature distribution.

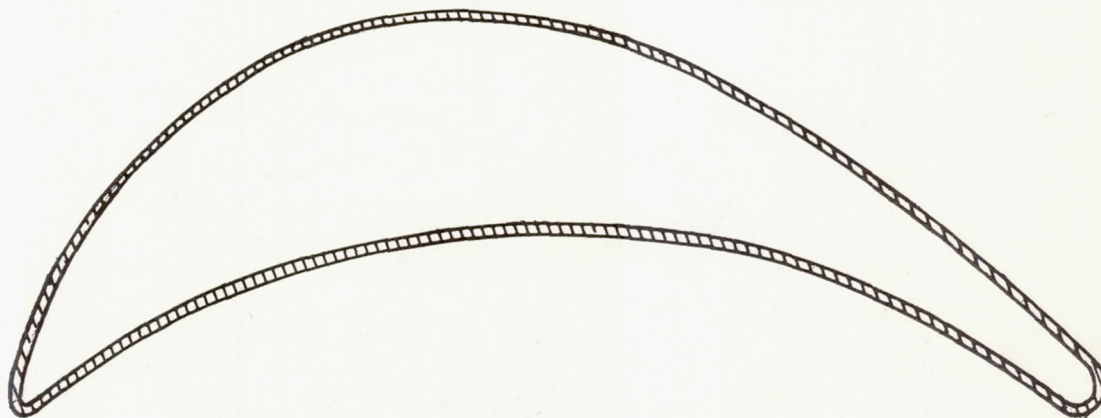


(b) Typical allowable stress distribution.

Figure 2. - Typical plots used to determine stress-ratio factors for air-cooled turbine rotor blade.



(a) Profile 1.



(b) Profile 2.



Figure 3. - Rotor blade profiles at midspan position for two blades considered. X3.

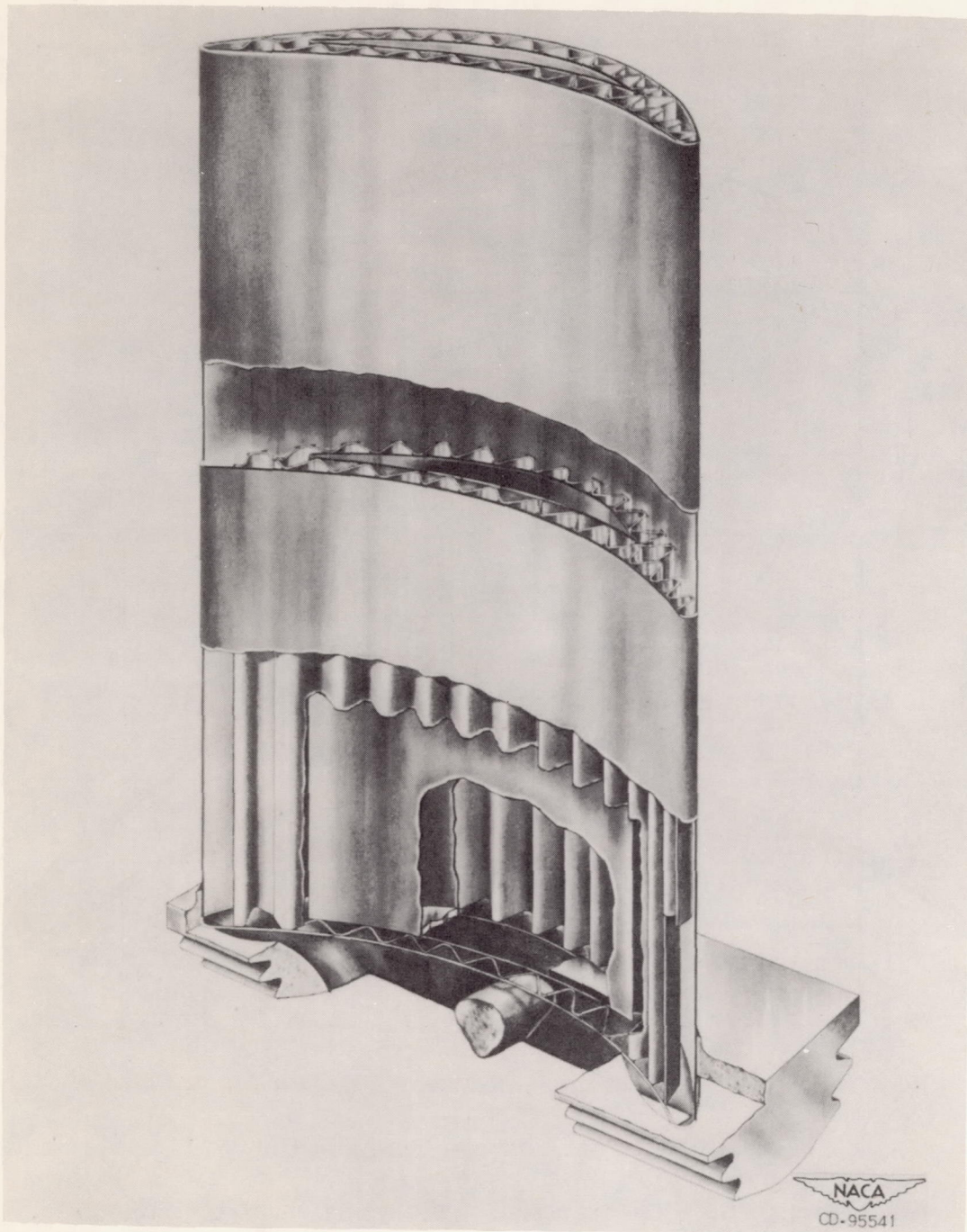
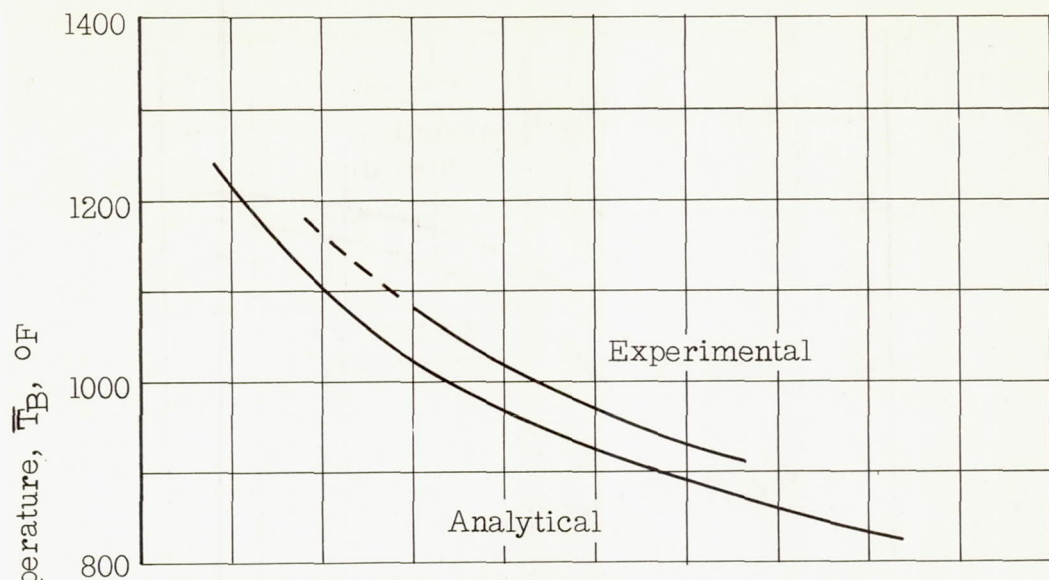
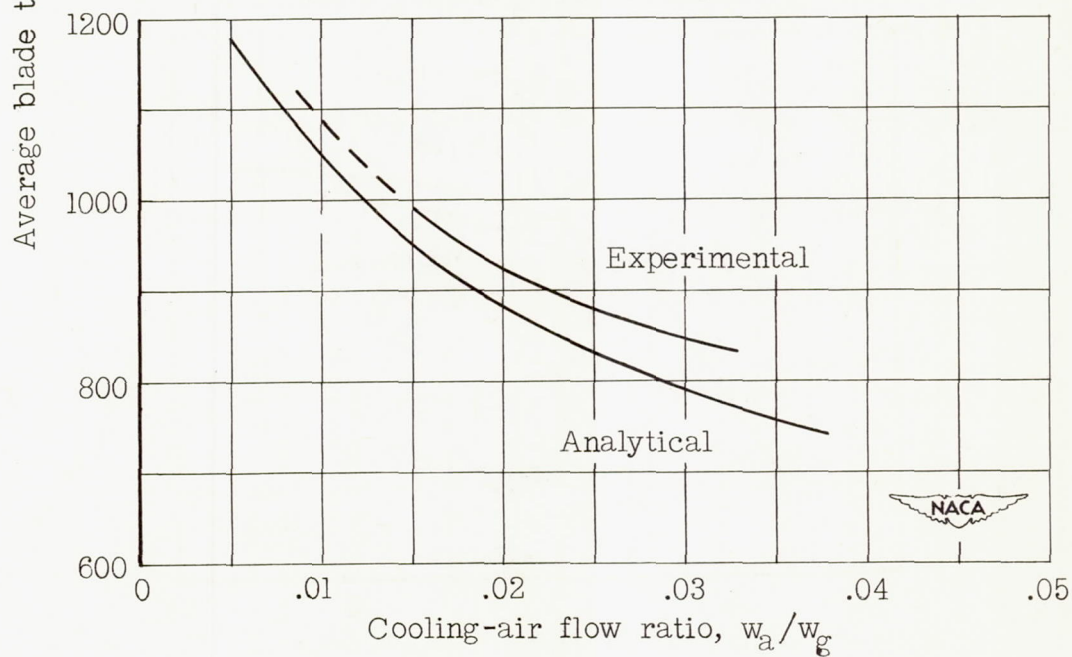


Figure 4. - Isometric sketch of air-cooled turbine rotor insert blade with fins.
Configuration H, profile 2.



(a) Coolant passage configuration A.



(b) Coolant passage configuration B.

Figure 5. - Comparison of analytical and experimental average blade temperatures at position $1\frac{7}{16}$ inches from blade root over range of cooling-air flow ratio for two coolant passage configurations of profile 1. Cooling-air temperature at blade root, 180° F.

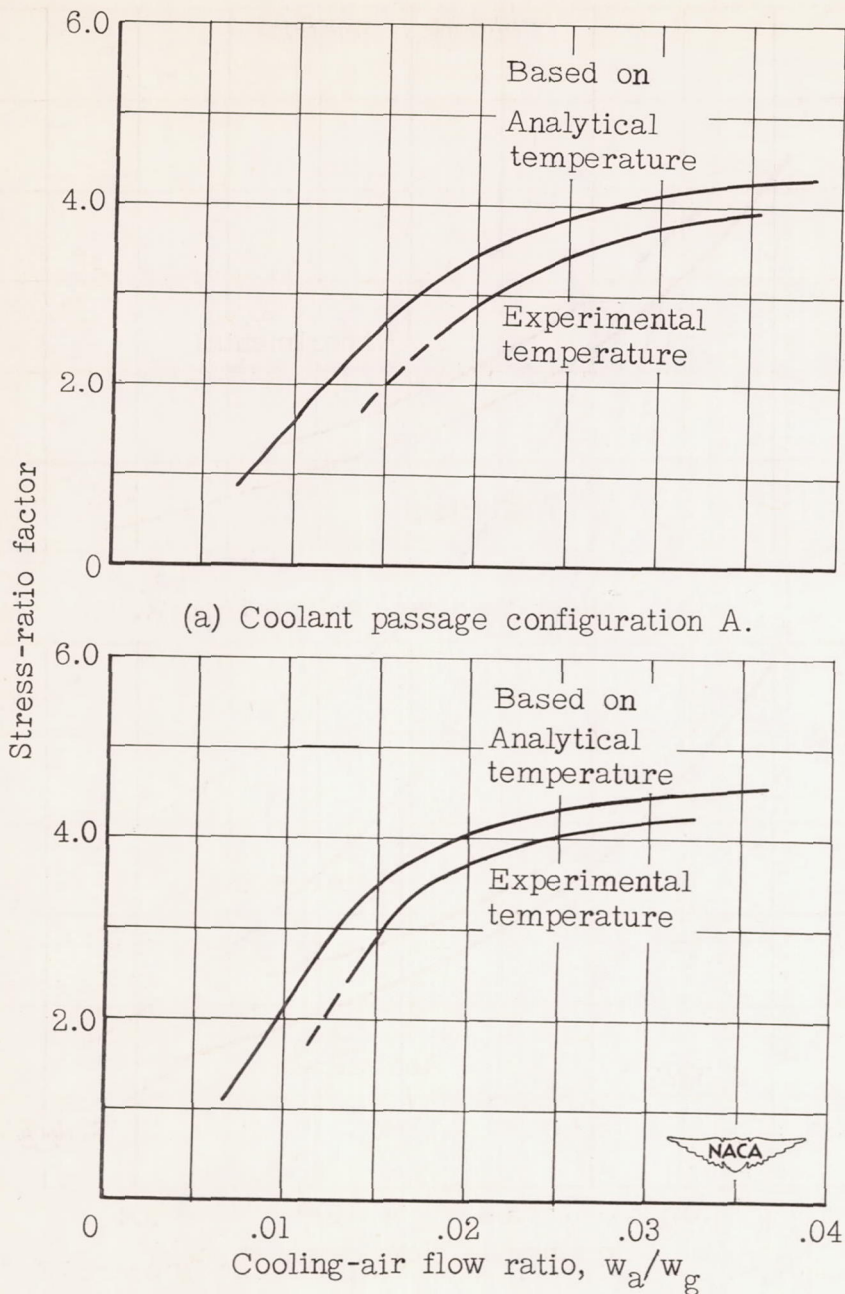


Figure 6. - Comparison of analytical and experimental stress-ratio factors at position $1\frac{7}{16}$ inches from blade root over range of cooling-air flow ratio for two coolant passage configurations of profile 1. Cooling-air temperature at blade root, 180° F.

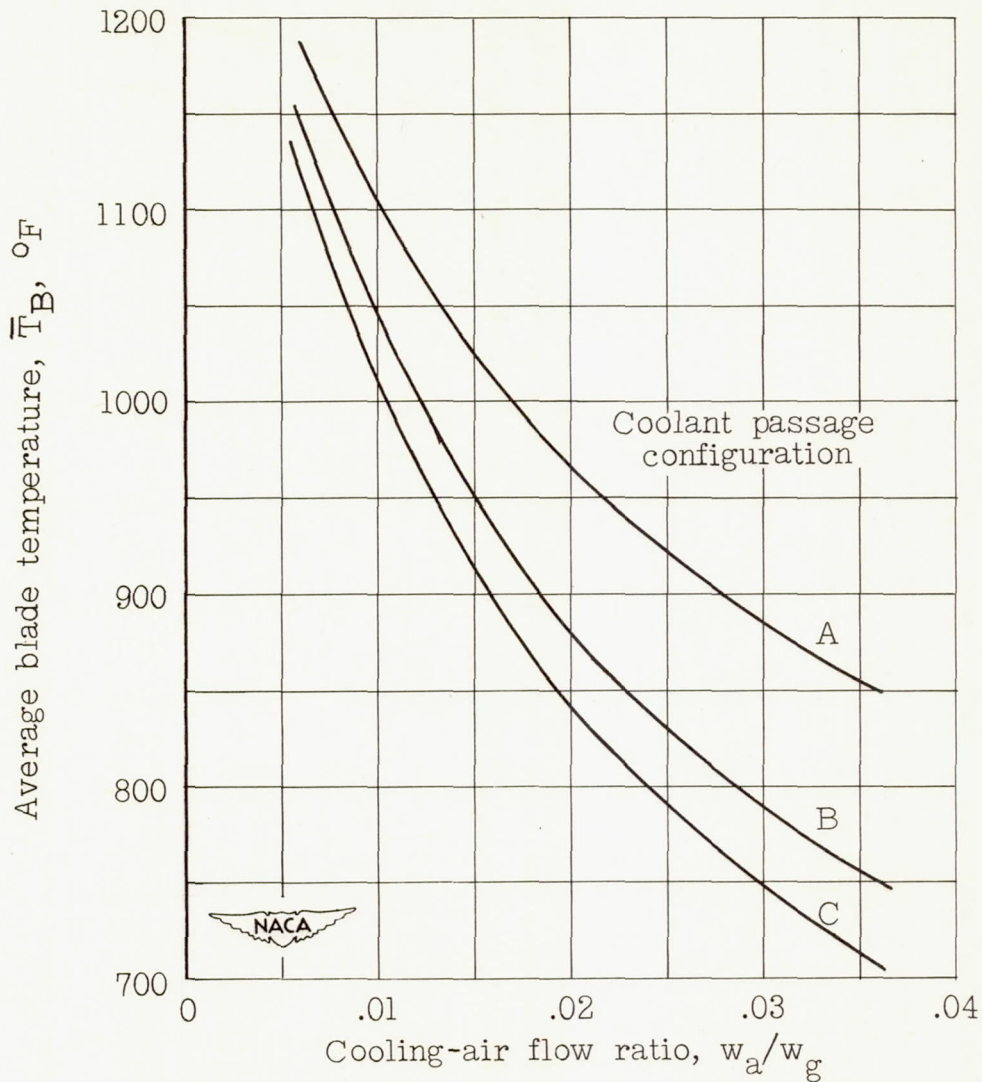


Figure 7. - Variation of average analytical blade temperature at position $1\frac{7}{16}$ inches from blade root with cooling-air flow ratio for three coolant passage configurations of profile 1. Cooling-air temperature at blade root, 180° F.

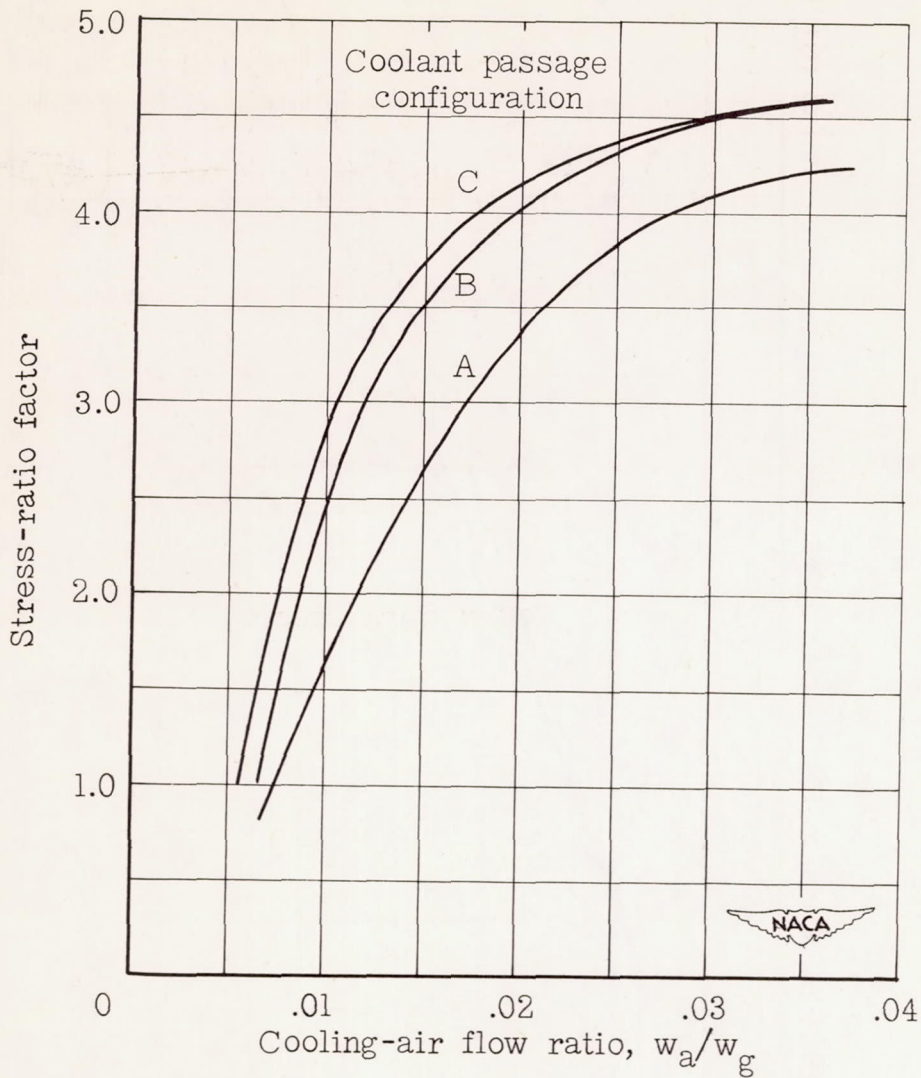


Figure 8. - Variation of stress-ratio factor based on average analytical blade temperatures at position $1\frac{7}{16}$ inches from blade root with cooling-air flow ratio for three internal passage configurations of profile 1. Cooling-air temperature at blade root, 180° F.

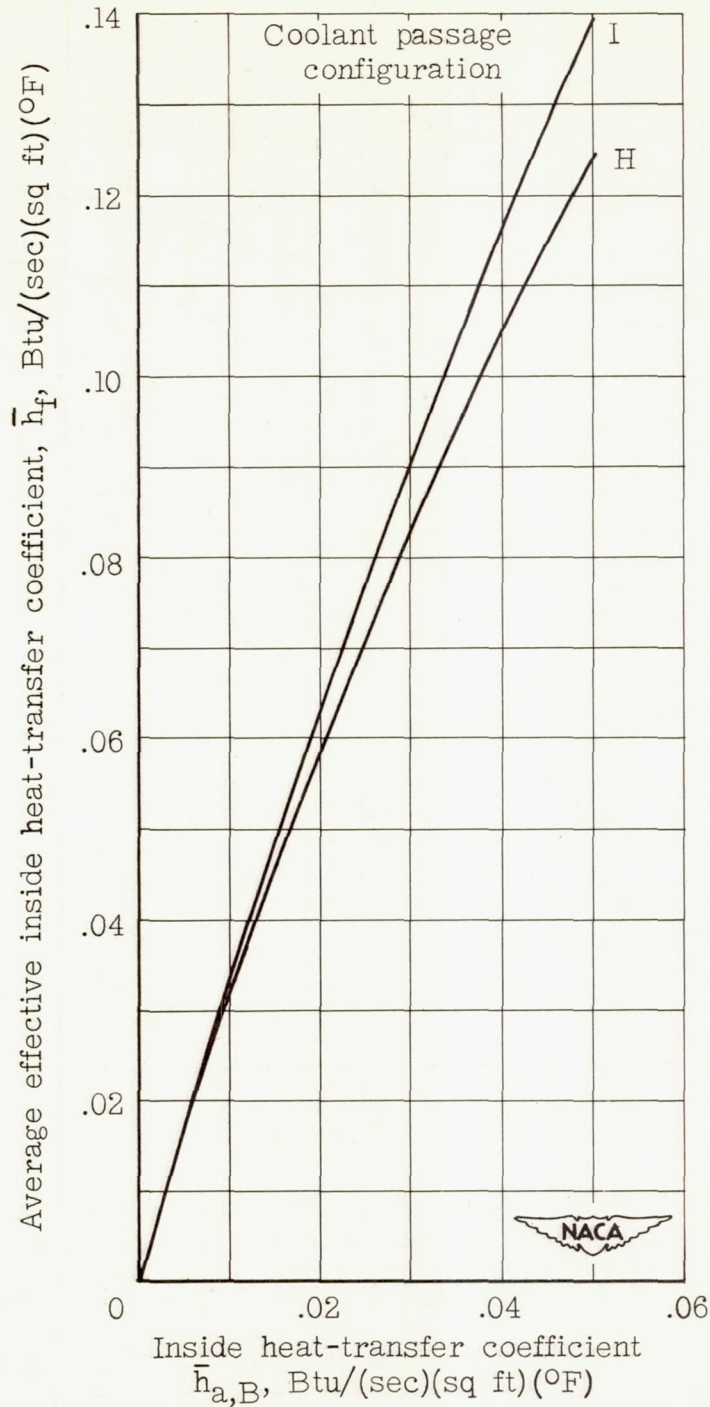


Figure 9. - Relation between average effective inside heat-transfer coefficient and inside-transfer coefficient for two coolant passage configurations of profile 2.

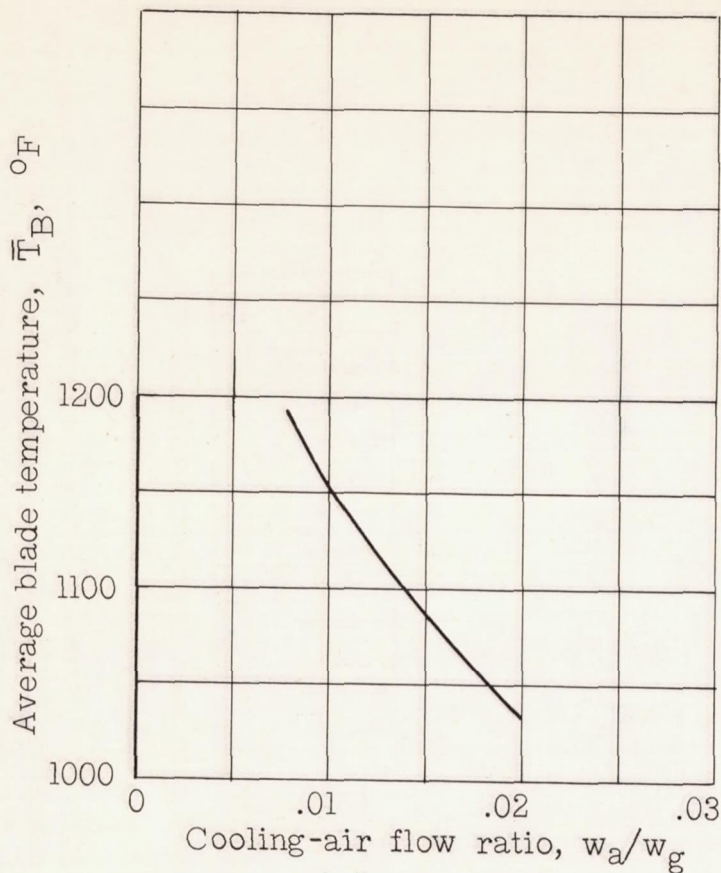


Figure 10. - Variation of average analytical blade temperature at position 1.5 inches from blade root with cooling-air flow ratio. Configuration H, profile 2. Cooling-air temperature at blade root, 180° F.

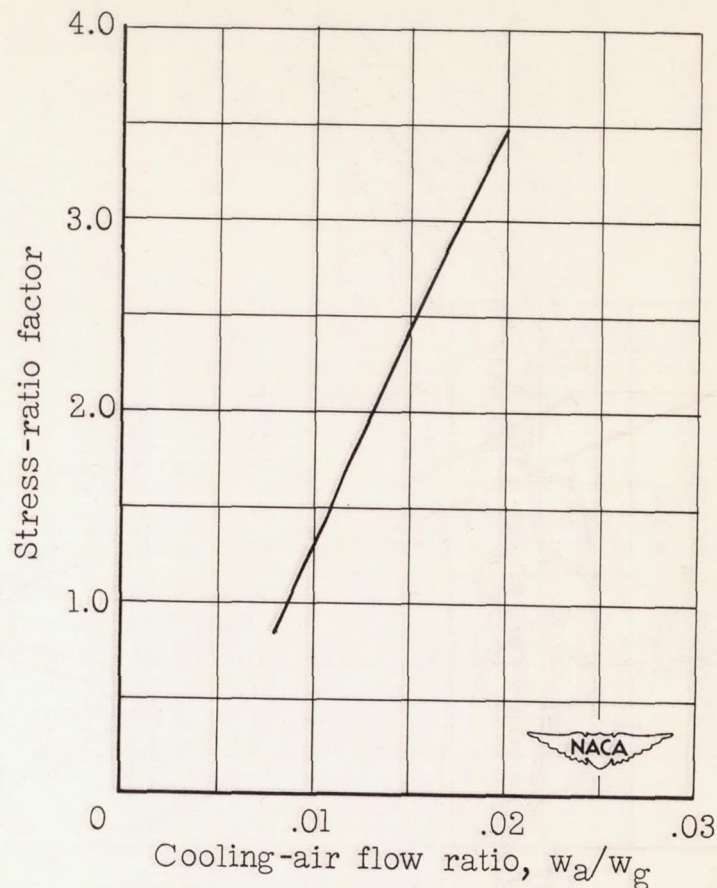
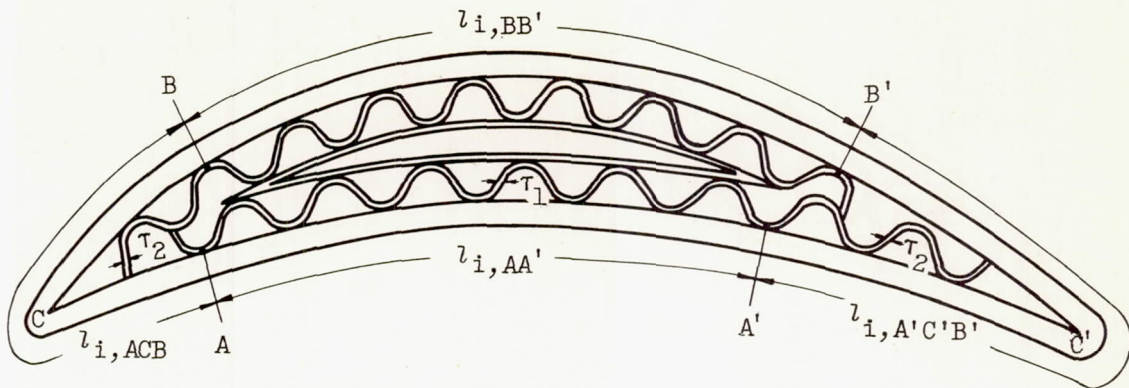
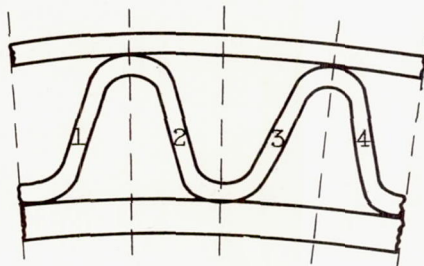


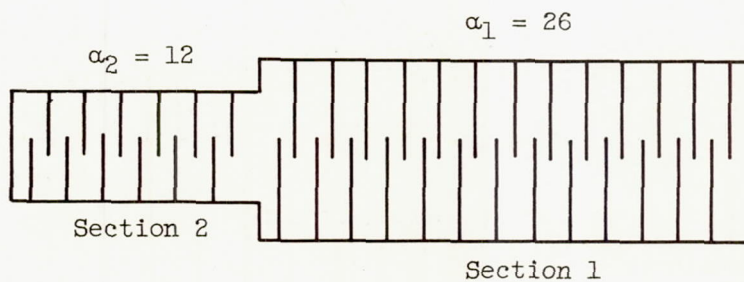
Figure 11. - Variation of stress-ratio factor based on average analytical blade temperature at position 1.5 inches from blade root with cooling-air flow ratio. Configuration H, profile 2. Cooling-air temperature at blade root, 180° F.



(a) Configuration B, profile 1.



(b) Typical section of coolant passage showing four equivalent fins.



(c) Equivalent fin sections.

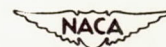
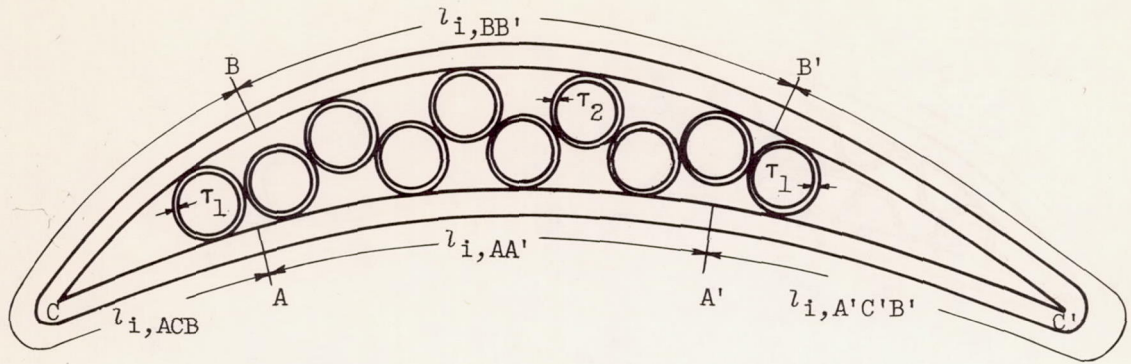
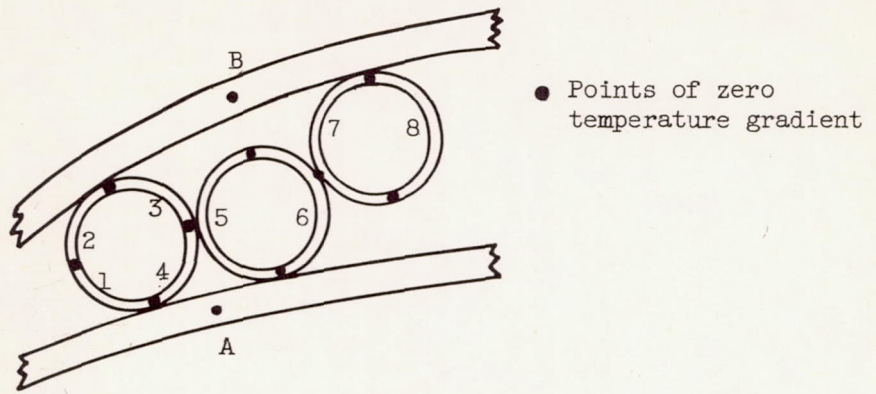


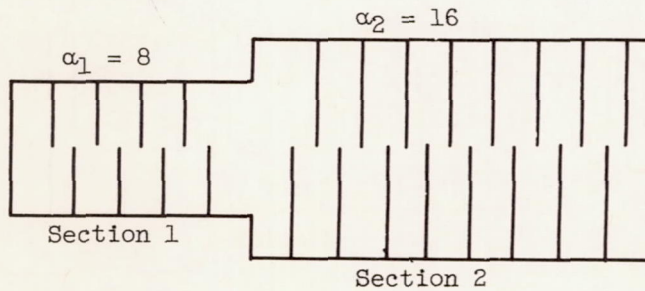
Figure 12. - Figures used for determining effective inside heat-transfer coefficient for configuration B, profile 1.



(a) Configuration A, profile 1.



(b) Section of coolant passage showing eight equivalent fins, four of section 1 and four of section 2.



(c) Equivalent fin sections.

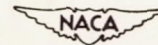


Figure 13. - Figures used for determining effective inside heat-transfer coefficient for configuration A, profile 1.